Ph.D. Thesis

SOMATOSENSORY EVOKED MAGNETIC FIELDS IN HUMANS

Motoko Shimojo

Department of Physiological Sciences,
School of Life Sciences,
The Graduate University for Advanced Studies

and

Department of Integrative Physiology,
National Institute for Physiological Sciences,

Myodaiji, Okazaki, Aichi 444-8585
JAPAN

1999

Contents

1. Preface

I studied neurophysiology, mainly magnetoencephalography (MEG), as a graduate student from April 1994 to March 1999 (including six months for maternity leave) in Professor Ryusuke Kakigi's Department, Department of Integrative Physiology, National Institute for Physiological Sciences, Okazaki, Japan. Compared to electroencephalography (EEG) which has been extensively examined and a largely used worldwide, MEG has several theoretical advantages in localizing brain activities because of fewer effects from the cerebrospinal fluid, skull and skin. In good conditions, spatial resolution of MEG is approximately 3-5 mm, and its temporal resolution is 1 msec. Therefore, MEG examination is one of the most useful and promising research themes. Professor Kakigi's Department is one of the pioneers of MEG study in Japan, and is now one of the world leaders in this field.

I mainly studied MEG results on somatosensory functions in humans, termed "somatosensory evoked magnetic fields (SEF)". By examining SEF, detailed functional anatomy of the primary and secondary somatosensory cortex (SI and SII) in humans have been elucidated in the last 10 years.

I summarized three of my previous studies on SEF, which were originally published in English, for this thesis.

2. Introduction

The magnetoencephalography (MEG) measures the magnetic fields which are originated from neurones in cerebral cortex non-invasively. The strength of the recorded MEG is approximately 50~1000fT, and these are reduced in anti-proportion to the square or cube of the distance from the sources. Therefore, it is necessary to use the well sensitive measuring instrument such as superconducting quantum interference device (SQUID). In an ideal condition, the spatial resolution of MEG is only a few mm which is over 10 times smaller than that of electroencephalography (EEG).

On the other hand, there are two major disadvantages of MEG. The first one is that MEG cannot detect the magnetic signals generated in the deep sites of brain, because the signals are rapidly reduced with a depth of the generator. EEG can measure the signal from deep area of the brain by volume conduction, although the spatial resolution is not so well, over a few cm. The second one is that MEG cannot measure the radial component of magnetic signals originated from the cerebral gyri, although it detects tangential component generated in the cerebral sulcus very well (Williamson et al., 1981).

Until 1983, only the single-channel MEG device was available. Since then, the number of channels was rapidly increased. In 1989, the 37-channels device, which was used for the present study, was produced. Recently, the new whole-head type MEG devices (over 100 channels) has appeared.

There have been a large number of papers reporting the somatosensory evoked potentials (SEPs) by averaging time-locked EEG. However, as compared with SEP (EEG), MEG has several theoretical advantages in localizing brain dipoles due to less skull effects and detection of only a specific orientation of brain current tangential to the skull as described above (Sutherling et al. 1992). Therefore, several investigators have been reporting

somatosensory evoked magnetic fields (SEFs) (Brenner et al., 1978; Hari et al., 1984; Huttunen et al., 1987; Rossini et al., 1989; Narich et al., 1991; Kakigi et al., 1995a, 1995b) by averaging time-locked MEG, and found activities around the first and second sensory cortices (SI and SII).

Among various research subjects of SEFs, I mainly focused on the following two themes; (1) Detailed receptive fields in the SI following stimulation of the various nerves of the lower limb, and (2) Intracerebral interactions caused by simultaneous stimulation of bilateral peripheral nerves, since these two subjects were not clearly elucidated yet. I report three studies in this thesis; Study I: Differentiation of receptive fields in the sensory cortex following stimulation of various nerves of the lower limb in man (Shimojo et al. 1996a), Study 2: Intracerebral interactions caused by bilateral median nerve stimulation in man (Shimojo et al. 1996b), and Study 3: Intracerebral interactions caused by bilateral posterior tibial nerve stimulation in man (Shimojo et al. 1997).

The main objective of these studies was to investigate the physiological functions of the human somatosensory system by using an excellent spatial and temporal resolution of MEG.

3. Methods

Subjects

Seven normal volunteers (five males and two females; mean age 34.4 years, range 29-42 years; mean height 167 cm) were studied. Informed consent was obtained from all participants to the study.

MEG device

SEFs were measured with dual 37-channel biomagnetometers (Magnes, Biomagnetic Technologies Inc., San Diego, CA). The detection coils of the biomagnetometer were arranged in a uniformly distributed array in concentric circles over a spherically concave surface. The device was 144 mm in diameter and its radius of curvature was 122 mm. The outer coils were 72.5° apart. Each coil was 20 mm in diameter and the distance of the center of each coil was 22 mm apart. Each coil was connected to SQUID. The measurement matrix was centred at five different positions, that is, around the C3, C4, Fz, Pz and Cz of the International 10-20 System in each subject. The C3 and C4 positions which covered SI and SII of the left and right hemisphere, respectively. The Fz, Cz and Pz position covered the frontal, central and parietal areas. The C3 and C4, and the Fz and Pz positions were recorded simultaneously using two probes, and the Cz position which covered the lower limb area of the SI was recorded using one probe. We selected the positions of MEG device depending on the research objectives.

Stimulus

The electric stimulus was a constant voltage square-wave pulse delivered transcutaneously to the trunk of the peripheral nerves. The stimulus duration was 0.3 msec.

In study I, The electric stimulus was delivered to four nerves of each lower limb unilaterally, posterior tibial nerve (PT) at the ankle, sural nerve

(SU) at the ankle, peroneal nerve (PE) at the knee and femoral nerve (FE) overlying the inguinal ligamentum, at a rate of 1/sec. Therefore, SEFs following stimulation of eight different nerves in each subject were recorded, and the difference among them was examined in 14 limbs of seven subjects. The stimulus intensity for the PT, PE and FE stimulation was decided individually to obtain sufficient stimulus strength to produce a definite movement of the corresponding muscles. The stimulus intensity for the SU stimulation was matched to give an equally strong sensation to the PT stimulation.

In Study II, the electric stimulus was delivered to the median nerve at the wrist at a rate of 1/sec. The intensity was sufficient to produce a definite twitch of the thumb.

In Study III, the electric stimulus was delivered to the posterior tibial nerve at the ankle at a rate of 1/sec. The intensity was sufficient to produce a definite twitch of the big toe.

Recording

The recordings were made in a magnetically shielded room in all three studies. Responses were filtered with a 0.1-200 Hz bandpass filter, and digitized at a sampling rate of 1012 Hz. The analysis time was 100 msec before and 600 msec after the stimuli, and DC was offset using a pre-stimulus period as the baseline. The recordings were made in a magnetically shielded room. The subject was sitting or lying on a bed depending on the recording area of the scalp, with eyes open.

Waveform analysis in Study II and III

As all components of SEFs showed polarity-reversal, the "amplitude" of each component was measured by adding the maximum amplitude of the outgoing and ingoing magnetic fields.

In Study II and Study III, the "right stimulation" waveform and "left stimulation" waveform were added to derive the "summated" waveform. The "bilateral" waveform was subtracted from the "summated" waveform to derive a "difference" waveform.

Analysis of equivalent current dipole (ECD)

A spherical model was fitted to the digitized head shape of each subject, and the location (x, y, z positions), orientation and amplitude of a best-fitting single equivalent current dipole (ECD) was estimated for each time point. We also adopted the software of double ECDs made by BTi (Lypchuk, 1991) in Study III, since the foot area of SI of each hemisphere is very closed each other. Yumoto et al. (1995) reported that the simulation study using this two ECD analysis demonstrated a position accuracy better than 3 mm, when two current dipoles were 3 cm beneath the surface and their distance was over 7 mm.

The origin of the head-based coordinate system was the midpoint between the preauricular points. The x-axis indicated the coronal plane with a positive value toward the anterior direction; the y-axis indicated the mid-sagittal plane with positive values toward the left preauricular point, and the z-axis lay on the transverse plane perpendicular to the x-y line with a positive value toward the upper side. "Correlation" and "goodness of fit" were calculated. The value of the former was the correlation between recorded measurements and the values expected from the ECD estimate. It was a report, in other words, of how closely the measured values corresponded to the theoretically expected values. Correlations between the theoretical field generated by the model and the observed field were used to estimate the goodness of fit of the model parameters. To ensure a strict criteria for dipole fitting, only estimates with a correlation and/or goodness of fit above 0.98 were analysed.

Superimposition of ECD on MRI

Magnetic resonance imaging (MRI) was obtained using a GE Signa 1.0 T system. The T1-weighted coronal and axial images with continuous 3 mm slice thickness were adopted for overlays with ECD sources detected by MEG. Using a recording matrix of 256X256 pixels, a field of view of 250mm, this sequence provides a plane resolution of 1X1mm in the slices. The same anatomical landmarks used to create the MEG head-based 3D co-ordinate system (the nasion and bilateral pre-auricular points) were visualised in the MR images by affixing to these points high contrast cod liver oil capsules (3mm diameter), whose short relaxation time provides a high signal in T1-weighted images. The common MEG and MRI anatomical landmarks allowed easy transformation of the head- based 3D co-ordinate system (nasion and entrance of the auditory meatus of the left and right ear) used by the MEG source analysis to the MRI. The MEG source locations were converted into pixels and slice values using the MRI transformation matrix and inserted onto the corresponding MRIs.

Statistical Analysis

Statistical analysis of the difference of the latency and amplitude and ECD location of each component was done by a paired t test, and $P<0.02$ was considered to be significant. As all components of SEFs showed polarity-reversal, the "amplitude" of each component was measured by adding the maximum amplitude of the outgoing and ingoing magnetic fields.

4. Results

Study I

The deflections less than 100 msec in latency recorded following stimulation of each nerve were generally similar in waveform, but the peak latency was different, mainly due to the difference of the stimulus site and stimulated fibers. Therefore, we termed each recognizable component, 1M, 2M, 3M and 4M for the first, second, third and fourth magnetic field, respectively (Fig. 1); their peak latency being about 37, 47, 58 and 76 msec, respectively, after PT stimulation. As described in detail previously (Kakigi et al., 1995b), independent minor deflection, with a latency about 3 msec longer than the 1M, was also clearly identified in about half of the subjects. They were marked by * in waveform following stimulation of PT and SU in Fig. 1. However, to avoid confusion, only major deflections were analyzed in the present study.

Peak Latency of 1M

The peak latency of the initial component, 1M, was the shortest following FE stimulation, and then they were prolonged following PE, PT and SU stimulation in this order (Table 1). Differences in peak latencies among each nerve stimulation were statistically significant (Table 2). The amplitude of the 1M was the largest following PT stimulation, and then they were reduced following SU, PE and FE stimulation in this order. The difference of amplitude between PT stimulation and others was significantly larger ($P<0.001$) (Tables 3 and 4). The amplitude of the 1M following SU stimulation was also significantly larger than that following FE stimulation. The difference of the 1M amplitude between PE and FE stimulation was not significant.

Peak Latencies of 2M, 3M, and 4M

The peak latencies and amplitudes of the following components, 2M, 3M and 4M, showed the same tendency, but the interindividual difference was large (Tables 1 and 3), and the statistical significance was gradually reduced (Tables 2 and 4). There was a small left-right difference in the peak latency and amplitude (Tables 1 and 3).

Estimated ECDs

The ECD of each deflection was estimated to be every 0.96 msec. The estimated ECD overlapped on MRI. All estimated ECD of the 1M, 2M, 3M and 4M components following each nerve stimulation was located on the hemisphere contralateral to the stimulated limbs. However, the location of ECD of the late- latency components, particularly 3M and 4M, was variable and was outside of the sensory cortex in studies of some limbs. This finding was probably due to the mixture of activities in various areas for such later components. In addition, we determined the differentiation of receptive fields following stimulation of various nerves. Therefore, we focused on the results of the 1M in the present study.

The ECD following the PT, SU and PE stimulation was located along the interhemispheric fissure in all 14 limbs. By contrast, the location of ECD following the FE stimulation was variable, on the crown of the postcentral gyrus, at the edge of the interhemispheric fissure or along the interhemispheric fissure. The distance of the ECD location of each component among each nerve was calculated (Table 5). The ECD location following PT stimulation was very close to that following SU and PE stimulation; the mean difference was approximately 1 cm. The difference of ECD location between FE stimulation and three other nerve stimulations was relatively large. For example, the mean of the distance of ECD between FE and SU was 1.71 cm, about 0.7 cm longer than that between PT and SU ($P<0.001$). By considering

the isocontour map and the distance of ECD of the 1M following each nerve stimulation, we classified the results of 14 limbs into two types (Table 6).

Results for Type 1

In type 1 (nine limbs), the distance of ECD between FE and PT stimulation was longer than 1 cm. The ECDs of the PT and SU stimulation were close to each other, but that of the FE stimulation was clearly isolated. The distance of ECDs between PT and FE was significantly ($P<0.01$) longer than that between PT and SU in type 1 (Table 6). ECD following PE stimulation was along the interhemispheric fissure in all 14 limbs like PT and SU, but its location was higher than that of PT and SU to some degree in type 1. The isocontour maps following PT, SU and PE stimulation were similar, in terms of the position of the maximal point of the ingoing and outgoing flux and the zero-point line, but that following the FE stimulation was much different (Fig. 2). The position of the ECD of the FE was on the crown of the postcentral gyrus or at the edge of the interhemispheric fissure, and it was directed to the posterior and inferior ward (Fig. 3). By contrast, the ECDs following stimulation of the other 3 nerves located along the interhemispheric fissure, and its direction was mainly horizontal, to the hemisphere ipsilateral to the stimulated nerve (Fig. 3). The distance of ECD between PT and PE stimulation was variable, for example it was small in Fig. 3, but the distance of ECDs between PE and FE was significantly ($P<0.01$) shorter than that between PT and FE in type 1 (Table 6).

Results for Type 2

In type 2 (five limbs), the distance of ECD between FE and PT stimulation was less than 1 cm, and the ECDs of each nerve stimulation were located relatively close to each other. Therefore, no significant difference in the distance of ECD was identified in type 2. However, the direction of ECD

of the FE and PE was different from that of PT and SU in five and two limbs, respectively. This difference was clearly recognized on the isocontour map (Fig. 4) and the axial plane of MRI (Fig. 5).

With regard to the intraindividual (left-right) difference, type 1 following each limb stimulation was found in two subjects, and the remaining five subjects showed type 1 following one limb stimulation and type 2 following stimulation of the other limb.

These findings are summarized as follows; (1) The magnetic fields caused by stimulation of PT and SU were similar in the results of all 14 limbs. (2) The location of ECDs following PE stimulation was between that of PT and SU and that of FE in type 1, and the direction of ECD following PE stimulation was clearly different from that of PT and SU in two limbs of type 2. (3) ECD following FE stimulation was clearly different from that of others, in terms of the location and/or direction, in the results of all 14 limbs. (4) The Inter- and intraindividual differences were frequently identified.

Study II

Unilateral stimulation

SEFs following unilateral median nerve stimulation in normal controls have been frequently described, and we have studied in detail the SEFs in normal controls using our magnetometer previously (Kakigi 1994; Kakigi et al. 1995a).

The C3 and C4 positions covered the primary and second sensory cortices (SI and SII, respectively) and their surrounding areas in the left and right hemisphere, respectively. Of the short- and middle-latency components of less than 70 msec, the main deflections, N20m-P30m-N40m-P60m, and their counterparts, P20m-N30m-P40m-N60m, were identified in the hemisphere contralateral to the stimulated nerve (contralateral hemisphere)

(Fig. 6). The nomenclature was based on the conventional EEG style using polarity and peak latency of each component. That is, N20M meant The ECDs of these deflections were identified around the hand area of the primary somatosensory cortex (SI), probably area 3b (Fig. 7). In the hemisphere ipsilateral to the stimulated nerve (ipsilateral hemisphere), small deflections were identified in each subject, but they were not consistent.

Of the deflections longer than 70 msec, particular deflections, N90m and P90m, were identified (Figs. 6 and 8) in bilateral hemispheres. The ECD position was around the superior bank of the Sylvian fissure, and its direction was more vertical than that of the previous ECDs generated in SI (Figs. 2 and 4). The generator site is considered to be the second sensory cortex (SII).

When the measurement matrix was centered at the Fz (mid-frontal), Cz (mid-central) and Pz (mid-parietal), the recordings revealed no significant responses which were independent of the responses described above, and no significant ECDs in those areas.

The "summated" waveform which was derived from a summation of the "right stimulation" and the "left stimulation" did not show any significant difference from the "unilateral stimulation" waveform. No significant difference in the "summated" waveform was observed between the two hemispheres, although the short- latency components appeared larger in the right hemisphere, and the middle-latency ones appeared larger in the left hemisphere (Tables 7 and 8).

Bilateral stimulation

The "bilateral" waveform identified in each hemisphere showed no consistent difference from each other, although the short-latency components appeared larger in the right hemisphere, and the middle-latency ones appeared larger in the left hemisphere (Tables 7 and 8). As compared with the "summated" waveform, peak latencies of each component were almost the

same between them (Table 7). Short-latency deflections of the "bilateral" waveform showed no significant difference in amplitude from that of the "summated" waveform. However, the N60m-P60m deflection was smaller in the "bilateral" waveform, particularly in the right hemisphere (C4 position) ($P<0.01$) (Table 8). The N90m-P90m in the "bilateral" waveform was clearly smaller than that in the "summated" waveform in each hemisphere in all subjects, and the difference was significant ($P<0.001$) (Table 8).

The difference between the "summated" and "bilateral" waveform was more clearly identified in the "difference" waveform (Fig. 8). The main deflection, U90m-D90m, was identified in all subjects. U and D indicate upward and downward deflection, respectively. As compared with the "summated" and "bilateral" waveform, the U90m-D90m showed broader duration starting from approximately 50 msec. Their ECDs were located around the superior bank of the Sylvian fissure, and their direction oriented mainly upward and anterior (Fig. 9). Their sites were similar to those of the N90m-P90m in the "summated" and "bilateral" waveform (Fig. 9). The recordings obtained for the measurement matrix centered at the Fz, Cz and Pz revealed no additional new findings to the previous descriptions like unilateral stimulated SEFs, and no consistent deflection was found in the "difference" waveform (Fig. 10).

Study III

Analysis of waveforms changes

The findings we obtained previously on the SEFs following unilateral posterior tibial nerve stimulation in normal controls using our magnetometer (Kakigi et al., 1995b; Shimojo et al., 1996a), and those obtained in this study were generally compatible with those reported from other institutes (Kaukoranta et al., 1986; Huttunen et al., 1987; Narich et al., 1991; Fujita et

al., 1995). Five deflections, N37m-P45m-N60m-P75m-P100m, and their counterparts, P37m-N45m-P60m-N75m-P100m, were identified (Fig. 11). N37m-P37m, P45m-N45m, N60m-P60m and N75m-P75m was consistent with 1M, 2M, 3M and 4M in Study I, respectively.

When the "bilateral" waveform was compared with the "summated" waveform, which was derived from a summation of the "right stimulation" and the "left stimulation", peak latencies of each component were similar between them (Table 9). Short-latency deflections of the "bilateral" waveform showed no significant change in amplitude from the "summated" waveform. However, the N100m-P100m in the "bilateral" waveform was clearly smaller than that in the "summated" waveform in all subjects, and the difference was significant ($P<0.02$) (Table 9).

The difference between the "summated" and "bilateral" waveform was more clearly identified in the "difference" waveform, in which the main deflection, U100m-D100m, was identified (Fig. 12). "U" and "D" meant upward and downward deflection, respectively. No consistent deflection was found except for the U100m-D100m in the "difference" waveform.

Source localization

According to the localization and direction of double ECDs in "bilateral" waveforms, the subjects were classified into two types, type 1 and type 2 (Fig. 13). In type 1 (four subjects), the ECDs in the two hemispheres were not close to each other (over 1 cm, mean 1.32 cm). However, in type 2, the ECDs in the two hemispheres were less than 1 cm (mean 0.70 cm) apart, and were in exactly the opposite direction. The isocontour maps showed the difference between type 1 and type 2 more clearly (Fig. 13). The maps in type 1 clearly depicted the two dipoles, but those in type 2 did not. The maps in type 2 rather revealed a single ECD with small amplitude. This finding was probably due to partial offset of magnetic fields generated in each

hemisphere. Similar findings as the "bilateral" waveform were also identified in "summated" waveform, that is, subjects classified into type 1 and 2 in "bilateral" waveform were also classified into type 1 and 2 in "summated" waveform, respectively.

ECDs of the N100m-P100m in "bilateral" and "summated" waveform were located around the superior bank of the Sylvian fissure, probably SII, in bilateral hemispheres using double ECD model, and it was directed vertically (Fig. 14). The isocontour maps and the location and direction of ECDs in both waveforms were fundamentally similar (Fig. 4). We have already reported that ECD of the N100m-P100m was located in the bilateral SII (Kakigi et al., 1995b), and we also found the same results when dual magnetometers were placed at the C3 and C4 positions.

5. Discussion

Study I

Unlike the hand area of the SI, the area of the lower limb in SI is located mainly in the bank along the interhemispheric fissure and the crown of the postcentral gyrus. Therefore, it is very difficult to determine the receptive fields following various nerves of the lower limb separately by non-invasive studies, mainly SEPs recording. When SEPs are recorded following stimulation of PT, the initial main response, the P37 corresponding to the 1M in the present study, appeared to be recorded in the hemisphere ipsilateral to the stimulated nerve, because the generator dipole directed horizontally to the hemisphere ipsilateral to the stimulated nerve. This particular finding is called "paradoxical lateralization" (Cruse et al., 1982; Lesser et al., 1987), a term which complicates its interpretation.

The receptive fields have been examined by analyzing the scalp topography of SEPs (Cruse et al., 1982; Desmedt and Bourguet, 1985; Guérit and Opsomer, 1991; Kakigi and Jones, 1986; Kakigi and Shibasaki, 1992; Kakigi and Shibasaki, 1983; Seyal et al., 1983; Tsuji and Murai, 1987; Tsumoto et al., 1972; Wang et al., 1989; Yamada et al., 1982). Wang et al. (1989) studied mapping following the FE stimulation in 10 subjects, and found that the initial component was maximal on the midline in all subjects. Its scalp distribution was clearly contralateral in six subjects, and restricted to the midline or slightly ipsilateral in four subjects. In other words, SEPs following stimulation of FE generally did not show the "paradoxical lateralization". However, even using such a method, it was impossible to determine the generator site in detail by the EEGs recording. Therefore, the MEG recording shown in the present study was very useful to solve this important problem. SEFs have been analyzed following lower limb

stimulation (Fujita et al., 1995; Hari et al., 1984; Huttunen et al., 1987; Kakigi et al., 1995b; Kaukoranta et al., 1986; Narich et al., 1991), but they have been studied only following stimulation of nerves at the ankle. Therefore, this is the first systematic report on the differentiation of the receptive fields of the lower limb area of SI by stimulation of many nerves at various sites.

The middle-latency deflections, 2M, 3M and 4M, were considered to be generated in SI like the 1M, but the location and direction of their ECDs were relatively variable and unstable as compared with those of the 1M, probably because of the effects of the activities from surrounding areas. Therefore, we will mainly discuss the 1M.

ECDs following stimulation of PT and the SN at the ankle were estimated around the middle of the bank of the interhemispheric fissure contralateral to the stimulated nerve, and fundamentally directed to the hemisphere ipsilateral to the stimulated nerve. The "paradoxical lateralization" can be clearly accounted for by the position and direction of their ECDs. The present finding was generally compatible with the previous studies (Fujita et al., 1995; Huttunen et al., 1987; Kakigi et al., 1995b; Kauloranta et al., 1986). The mean difference of the ECD position between the PT and SU was approximately 1 cm. Therefore, the receptive fields for these two nerves were considered to be very close or overlapping. Huttunen et al.(1987) reported that the mean difference in ECD location of those two nerves was 1.1 cm which was very similar to our present findings.

The ECD location following stimulation of the PE at the knee was between that following PT and SU stimulation and that following FE stimulation in type 1. This finding might indicate that the receptive fields to the ankle and knee stimulation were clearly separated in such particular limbs as shown in "homunculus". In type 2, ECDs were close to those following stimulation of PT and SU at the ankle, but its direction was apparently different from that of PT and SU in two limbs. The results in two such limbs

might indicate the independence of the receptive fields to PE from others. The amplitude of SEFs following PE was smaller than that of the PT, although its motor threshold was much lower than that of PT. This finding may have been due to a large movement of the leg produced by stimulation of the PE, because such movements caused reduction in amplitude of the cortical responses, named "gating" effects (Kakigi et al., 1994; Kakigi et al., 1995a).

The ECD following FE stimulation was located on the crown of the post-central gyrus or at the edge of the interhemispheric fissure in the study of nine out of 14 limbs (type 1), and the distance of ECD location between FE and other nerves was significantly large. This indicated that differentiation of the receptive fields in the area of the lower limb of SI were compatible with the homunculus in approximately 65 % (9/15) of the limbs. The ECD following FE stimulation located along the interhemispheric fissure in five other limbs. However, even when it was close to the ECD following stimulation of the other nerves, its direction was apparently different from that of others. This finding indicated the definite independence of the receptive fields following FE stimulation, and could account for the large different EEG mapping following FE stimulation from stimulation of the other nerves at the ankle (Wang et al., 1989).

In conclusion, MEG was a very useful method for detecting the differentiation of the receptive fields of the lower limb in SI non-invasively in humans. The present findings indicated that approximately 65% of the limbs show the particular receptive fields compatible with the homunculus. Even in the other 35%, the magnetic fields following stimulation of the PE and/or FE showed an apparent differentiation from those following the PT and SU. Not only the interindividual difference but also an intraindividual difference was recognized. This is probably due to the anatomical variation of the area of the lower limb in SI in humans.

Study II

SEPs following stimulation of bilateral median nerves have been used in clinical applications, mainly to reduce the recording time (Yamada et al., 1978, 1983). Recorded waveforms in each hemisphere are symmetrical in normal subjects. It was judged to be abnormal, when definite asymmetrical findings were identified in the patient. However, no detailed systematic study, except for that reported by Okajima et al. (1990), has been reported concerning the effects of bilateral simultaneous stimulations on the activations of the sensory cortices in each hemisphere, because it is difficult to deny the effects of volume conduction of the activities generated in the other hemisphere. Study of SEFs should be useful, because it can detect precisely localized cortical activities, particularly deflections in SII (Hari et al., 1984; Nambu and Matsuzaki, 1993; Kakigi, 1994; Kakigi et al., 1995).

Short-latency components which are considered to be generated in SI showed no significant difference between "summated" and "bilateral" waveforms. This indicated that early activities in SI in one hemisphere were not affected by those in the other hemisphere through volume conduction or interhemispheric conduction mediated through the corpus callosum. These findings were consistent with that of previous studies that sensory cortical areas associated with the extremities of the body do not appear to project to the other hemisphere via the corpus callosum in monkeys (Jones and Powell, 1969a,b; Karol and Pandya, 1971; Pandya and Vignolo, 1969), and are also consistent with those of studies of SEPs (Kakigi, 1986; Lueders et al., 1983) and SEFs (Hari et al., 1984; Kakigi, 1994) in humans.

The middle-latency component, the N60m-P60m, in the "bilateral" waveform was smaller than that in the "summated" waveform, although the difference was significant only in the right hemisphere. Iwamura et al. (1994) reported the presence of neurons which receive somatosensory signals from bilateral hands in the postcentral somatosensory cortex, areas 2 and 5, in the

monkey. Allison et al. (1989) reported that ipsilateral SEPs, with an onset latency of 40-50 msec, were recorded of the cortical surface in less than half of humans, and they considered that their generators were located in areas 4, 2 and 7. These findings may indicate that the decrease of the N60m-P60m was due to the effects of activities of such bilateral responses, although no consistent N60m-P60m was identified in the ipsilateral hemisphere. The reason why the difference was much larger in the right hemisphere remains unknown.

Significant differences in long-latency deflections were identified between "summated" and "bilateral" waveforms, the responses appearing were inhibited in the "bilateral" session. Then the U90m-D90m was identified in the "difference" waveform. The ECDs of the U90m-D90m were located around the superior bank of the Sylvian fissure in bilateral hemispheres. The SII was considered to be located around there in monkeys (Whitzel et al., 1969; Jones and Powell, 1970) and cats (Robinson, 1973). Since Penfield and Jasper (1954) reported the existence of SII in humans based on the results of a cortical stimulation study, Lüders et al. (1985) and Allison et al. (1989) reported the somatosensory evoked potentials recorded from SII following median nerve stimulation, using chronically implanted subdural electrodes (Lüders et al., 1985) or by direct recording from the cortical surface during surgery (Allison et al., 1989). Moreover, in recent MEG studies, current dipoles were detected which were considered to be generated in SII following median nerve stimulation (Hari et al., 1984; Nambu and Matsuzaki, 1993.; Kakigi, 1994; Kakigi et al., 1995). Therefore, it is considered that activities in neurons in SII were interfered when bilateral median nerves were stimulated.

Neurons in SII differ from those in SI in that their receptive fields are larger, encompassing ipsilateral as well as contralateral areas of the body surface for 63 % of the units studied in unanesthetized cats (Robinson, 1973) and 90 % of the units in unanesthetized monkeys (Whitzel et al., 1969). Jones

and Powell (1969a,b, 1970), reviewing previous papers, suggested that SII is an area for interhemispheric convergence of sensory input of all somatic modalities at a relatively low level of cortical function. Therefore, it seems appropriate that some particular interactions take place in SII following bilateral side stimulation. In the cat medial geniculate body, inhibition of the responses of some neurons was induced by simultaneous binaural stimulation with equal intensity at each ear as compared with monaural stimulation (binaural occlusion) (Aitkin and Dunlop, 1968). Similar occlusion may take place in SII in humans following bilateral median nerve stimulation.

Huttunen et al. (1992) reported observing inhibitory changes of SEFs following median nerve stimulation which was stimulated 40 msec after a conditioning ipsilateral ulnar nerve stimulation. For comparison, they also used the contralateral median nerve as the conditioning stimuli, but did not find any significant changes in the SEFs. Since their objective was to determine the effects of the previously applied conditioning stimulation of the median and ulnar nerves on SEFs following stimulation of the ipsilateral median nerve, they did not study the interactions following simultaneous bilateral median nerve stimulation.

Okajima et al. (1990) reported the interactions of SEPs following simultaneous bilateral stimulation, although they placed electrodes at only three sites, C3, C4 and Cz. They did not find any consistent components which appeared to correspond to our U90m-D90m, probably because it is very difficult to detect in EEGs components generated in SII. In contrast, they found three long-latency components longer than 100 msec in latency only from the Cz electrode, but no such components corresponding to them were identified in our SEF study. This indicated that long-latency SEPs being maximal around the Cz electrode are probably recorded by a summation of activities generated in multiple areas or in deep areas, but they could not be correctly detected by MEGs.

Study III

The results were generally similar to those in Study II. That is, the late components which were generated in the bilateral SII were significantly reduced in amplitude by bilateral simultaneous stimulation of the posterior tibial nerves. Underlying mechanisms of the results are considered to be the same as those speculated for median nerve stimulation (Study II).

The biggest new finding of this study was the usefulness of the double dipole mode. When bilateral nerves are stimulated, the two dipole model is necessary. To solve this problem, the dipole analysis method at one moment (Henderson et al., 1975; Lypchuk, 1991; Yumoto et al., 1995) and the spatio-temporal dipole model with fixed dipoles, for example brain electric source analysis (BESA) (Scherg and Berg, 1995), are the two leading methods. We now use these two methods properly depending on the waveform in terms of source location, latency or duration of each component. We used the former method in the present study, because of the vary close temporal difference and source location of the two dipoles.

The two dipoles in the two hemispheres were clearly identified following bilateral posterior tibial nerve stimulation. To our knowledge, this is the first report to show the difference of receptive fields in each hemisphere by simultaneous stimulation of bilateral lower limbs. We recently reported detailed studies on MEGs following posterior tibial nerve (Kakigi et al., 1995b) and femoral, sural and peroneal nerves (Shimojo et al., 1996b), and found that the receptive fields in SI to lower limb stimulation showed not only differences with the individual, but also within the individual, that is, the left-right difference. Here, we confirmed this finding in more detail, that is, subjects were classified into type 1 and type 2 according to the localization and direction of the two dipoles. In type 1, the magnetic fields generated by the two dipoles were clearly depicted, because the ECDs were not located close to each other. However, in type 2, the dipoles in the two hemispheres

were very close and in exactly the opposite direction. Therefore, the magnetic fields generated by the two dipoles appeared to be generated by a single dipole on the midline. We must be careful of such a phenomenon when we analyse SEPs or SEFs following bilateral lower limb stimulation.

General Discussion

These three studies clearly indicated the advantages of MEG recording in terms of extremely high spatial and temporal resolution. Particularly, acquirement of detailed temporal processing of information transferring in order of msec is the biggest advantage of MEG as compared with functional MRI (fMRI) or positron emission tomography (PET). In addition, MEG studies detect physiological neuronal activities rather than the change of metabolism or blood flow. A difference of ECD orientation which was found in Study 1 cannot be identified by fMRI or PET, since they indicated only the location of activities. A presence of SII in humans were not clearly recognised before the reports of MEG (Hari et al., 1984). Since then, location and function of human SII have been investigated by MEG (Hari et al., 1984; Kakigi, 1994; Kakigi et al., 1995). The unique findings identified in the present studies by simultaneous stimulation of the bilateral nerves also added new characteristics of SII neurones in humans.

In conclusion, usefulness of non-invasive study of human somatosensory system using MEG (SEFs) is confirmed, and the future studies of SEFs should be promising by changing a stimulation methods and/or paradigms.

6. Summary

We investigated in a magnetoencephalographic study that 1) the receptive fields following stimulation of the lower limb nerves (PT, SU, PE and FE), 2) intracerebral interactions in the brain caused by bilateral tibial nerve (lower limb) stimulation and bilateral median nerve (upper limb) stimulation. Approximately 65% of the limbs show the particular receptive fields compatible with the homunculus. Even in the other 35%, the magnetic fields following stimulation of the PE and/or FE showed an apparent differentiation from those following the PT and SU. Not only the interindividual difference but also an intraindividual difference was recognized. This is probably due to the anatomical variation of the area of the lower limb in SI in humans.

There was same tendency between the upper limb (median nerve) and the lower limb (tibial nerve), when they were stimulated bilaterally and simultaneously. Short-latency components, which are considered to be generated in SI, demonstrated no significant difference between "summated" and "bilateral" waveforms, but the long-latency ones generated in bilateral SII were significantly inhibited by bilateral stimulation, probably due to some interference effects, because neurons in SII receive inputs from bilateral sides of body.

7. Acknowledgements

The present Ph.D. thesis is based on work which I could not have performed without the support from many people. First of all I would like to express my sincere gratitude to Professor Ryusuke Kakigi for his never ending enthusiastic supervision. Furthermore, the collaborators in our Department are kindly acknowledged for support. I would like to give my special thanks to Mr. Osamu Nagata and Mr. Yasuyuki Takeshima, technicians in the Department of Integrative Physiology for helping and support.

The present work has been supported by the Uehara Memorial Foundation and the Naito Foundation in Japan, The Integrative Studies on Physiological Functions (06NP0101), Science and Culture of Japan, Magnetic Health Science Foundation and the Daiko Foundation and by a Grant-In-Aid for Scientific Research (07458215), for Scientific Research on Priority Areas (08279244) and for The Ministry of Education, Science, Sports and Culture of Japan.

8. References

Aitkin, L.M., and Dunlop, C.W. Interplay of excitation and inhibition in the cat medial geniculate body. J. Neurophysiol. 31 (1968) 44-61.

Allison, T., McCarthy, G., Wood, C.C., Williamson, P.D. and Spencer, D.D. Human cortical potentials evoked by stimulation of the median nerve, II. Cytoarchitectonic areas generating long-latency activity. J. Neurophysiol. 62 (1989) 711-722.

Baumgartner, C., Sutherling, W.W., Di, S. and Barth, D.S. Spatiotemporal modeling of cerebral evoked magnetic fields to median nerve stimulation. Electroencephalogr. Clin. Neurophysiol. 79 (1991) 27-35.

Brenner, D., Lipton, J., Kaufman, L. and Williamson, S.J. Somatically evoked fields of the human brain. Science, 189 (1978) 81-83.

Cruse R., Klem, G., Lesser, R.P. and Lüeders, H. Paradoxical lateralization of cortical potentials evoked by stimulation of the posterior tibial nerve. Arch. Neurol. 39 (1982) 222-225.

Desmedt, J.E. and Bourguet, M. Color imaging of parietal and frontal somatosensory potential fields evoked by stimulation of median or posterior tibial nerve in man. Electroencephalogr. Clin. Neurophysiol. 62 (1985) 1-17.

Fujita, S., Nakasato, N., Matani, A., Tamura, I. and Yoshimoto, T. Short latency somatosensory evoked field for tibial nerve stimulation: Rotation of dipole pattern over the whole head. In Baumgartner, G., Deecke, L., Stronik, G. and Williamson, S.J. (Eds.): Biomagnetism: Fundamental Research and Clinical Applications. Proceedings of the 9th International Conference on Biomagnetism, Studies in Applied Electromagnetics and Mechanics. Vienna: Elsevier 7 (1995) 95-98.

Guérit, J.M. and Opsomer, R.J. Bit-mapped imaging of somatosensory evoked potentials after stimulation of the posterior tibial nerve of the penis/clitoris. Electroencephalogr. Clin. Neurophysiol. 80 (1991) 228-237.

Hari, R., Reinikainen, K., Kaukoranta, E., Hämäläinen, M., Ilmoniemi, R., Penttinen, A., Salminen, J. and Teszner, D. Somatosensory evoked cerebral magnetic fields from SI and SII in man. Electroencephalogr. Clin. Neurophysiol. 57 (1984) 254-263.

Henderson, C.J., Butler, S.R. and Glass, A. The localization of equivalent dipoles of EEG sources by the application of electrical field theory. Electroenceph. clin. Neurophysiol. 39 (1975) 117-130.

Hoshiyama, M., Kakigi, R., Koyama, S., Kitamura, Y., Shimojo, M. and Watanabe, S. Somatosensory evoked magnetic fields after mechanical stimulation of the scalp in humans. Neurosci. Lett. 195 (1995) 29-32.

Hoshiyama, M., Kakigi, R., Koyama, S., Kitamura, Y., Shimojo, M. and Watanabe, S. Somatosensory evoked magnetic fields following stimulation of the lip in humans. Electroenceph. Clin. Neurophysiol. 100 (1996) 96-104.

Huttunen, J., Kaukoranta, E. and Hari, R. Cerebral magnetic responses to stimulation of tibial and sural nerves. J. neurol. Sci. 79 (1987) 43-54.

Huttunen, J., Ahlfors, S. and Hari, R. Interaction of afferent impulses in the human primary sensorimotor cortex. Electroencephalogr. Clin. Neurophysiol. 82 (1992) 176-181.

Iwamura, Y., Iriki, A. and Tanaka, M. Bilateral hand representation in the postcentral cortex. Nature, 369 (1994) 554-556.

Jones, E.G. and Powell, T.P.S. Connexions of the somatic sensory cortex of the rhesus monkey. I. Ipsilateral cortical connexions. Brain, 9 (1969a) 477-502.

Jones, E.G. and Powell, T.P.S. Connexions of the somatic sensory cortex of the rhesus monkey. II. Contralateral cortical connexions. Brain, 92 (1969b) 717-730.

Jones, E.G. and Powell, T.P.S. An anatomical study of converging sensory pathways within the cerebral cortex of the monkey. Brain, 93 (1970) 793-820.

Kakigi, R. and Shibasaki, H. Short-latency somatosensory evoked spinal and scalp-recorded potentials following posterior tibial nerve stimulation in man. Electroenceph. Clin. Neurophysiol. 53 (1982) 602-611.

Kakigi, R. and Shibasaki, H. Scalp topography of the short latency somatosensory evoked potentials following posterior tibial nerve stimulation in man. Electroencephalogr. Clin. Neurophysiol. 56 (1983) 430-437.

Kakigi, R. Ipsilateral and contralateral SEP components following median nerve stimulation. effects of interfering stimuli applied to the contralateral hand. Electroencephalogr. Clin. Neurophysiol. 64 (1986) 246-259.

Kakigi, R. and Jones, S.J. Influence of concurrent tactile stimulation on somatosensory evoked potentials following posterior tibial nerve stimulation in man. Electroencephalogr. Clin. Neurophysiol. 65 (1986) 118-129.

Kakigi, R. and Shibasaki, H. Effects of age, gender, and stimulus side on the scalp topography of somatosensory evoked potentials following posterior tibial nerve stimulation. J. Clin. Neurophysiol. 9 (1992) 431-440.

Kakigi, R. Somatosensory evoked magnetic fields following median nerve stimulation. Neurosci. Res. 20 (1994) 165-174.

Kakigi, R., Koyama, S., Hoshiyama, M., Watanabe, S., Shimojo, M. and Kitamura, Y. Gating of somatosensory evoked responses during active finger movements: magnetoencephalographic studies. J. Neurol. Sci. 121 (1995a) 195-204.

Kakigi, R., Koyama, S., Hoshiyama, M., Shimojo, M., Kitamura, Y. and Watanabe, S. Topography of somatosensory evoked magnetic fields following posterior tibial nerve stimulation. Electroenceph. Clin. Neurophysiol. 95 (1995b) 127-134.

Kakigi, R., Koyama, S., Hoshiyama, M., Shimojo, M., Kitamura, Y., Watanabe, S. and Nakamura, A. Effects of tactile interference stimulation on somatosensory evoked magnetic fields. NeuroReport, 7 (1996) 405-408.

Karol, E.A. and Pandya, D.N. The distribution of the corpus callosum in the rhesus monkey. Brain, 94 (1971) 471-486.

Kaufman, L., Okada, Y., Brenner, D. and Williamson, S.J. On the relation between somatic evoked potentials and fields. Int. J. Neurosci. 15 (1981) 223-239.

Kaukoranta, E., Hari, R., Hämäläinen, M. and Huttunen, J. Cerebral magnetic fields evoked by peroneal nerve stimulation. Somatosens. Res. 3 (1986) 309-321.

Kitamura, Y., Kakigi, R., Hoshiyama, M., Koyama, S., Shimojo, M. and Watanabe, S. Pain-related somatosensory evoked magnetic fields. Electroenceph. Clin. Neurophysiol. 95 (1995) 463-474.

Kitamura, Y., Kakigi, R., Hoshiyama, M., Koyama, S., Shimojo, M. and Watanabe, S. Effects of sleep on somatosensory evoked responses in human: a magnetoencephalographic study. Cogn. Brain Res. 4 (1996) 275-279.

Kitamura, Y., Kakigi, R., Hoshiyama, M., Koyama, S., Shimojo, M. and Watanabe, S. Pain-related somatosensory evoked magnetic fieldsfollowing lower limb stimulation. J. Neurol. Sci. 145 (1997) 187-194.

Lesser, R.P., Lueders, H., Hahn, J., Morris, H., Wyllie, E. and Resor, S. The source of 'paradoxical lateralization of cortical evoked potentials to posterior tibial nerve stimulation. Neurology, 37 (1987) 82-88.

Lueders, H., Lesser, R.P., Hahn, J., Dinner, D.S. and Klem, G. Cortical somatosensory evoked potentials in response to hand stimulation. J. Neurosurg. 58 (1983) 885-894.

Lüders, H., Lesser, R.P., Dinner, D.S., Hahn, J.F., Salanga, V. and Morris, H.H. The second sensory areas in humans: evoked potential and electrical stimulation studies. Ann. Neurol. 17 (1985) 177-184.

Lypchuk, T.A. Stabilization the nonlinear inverse problem for two dipoles in a sphere. In: Book of Abstracts of the 8th International Conference on Biomagnetism in Münster (1991) 87-88.

Nambu, A. and Matsuzaki, R. Neuromagnetic responses in the primary and secondary somatosensory cortices in human subjects. Jpn. J. Physiol. 43 (1993) 214.

Narich, L., Madonna, I., Opsomer, R.J., Pizzella, V., Romani, G.L., Torrioli, G., Traversa, R. and Rossini, P.M. Neuromagnetic somatosensory homunculus: a non-invasive approach in humans. Neurosci. Lett. 121 (1991) 51-54.

Okajima, Y., Chino, N., Saitoh, E. and Kimura, A. Interactions of somatosensory evoked potentials: simultaneous stimulation of two nerves. Electroencephalogr. Clin. Neurophysiol. 80 (1990) 26-31.

Pandya, D.N. and Vignolo, L.A. Interhemispheric projections of the parietal lobe in the rhesus monkey. Brain Res. 15 (1969) 49-65.

Penfield, W. and Jasper, H. Epilepsy and the functional anatomy of the human brain. J. and A. Churchill, London. (1954).

Penfield W, Rasmussen T: The Cerebral Cortex of Man. A Clinical Study of Localization of Function. New York: The Macmillan Company (1955).

Robinson, D.L. Electrophysiological analysis of interhemispheric relations on the second somatosensory cortex of the cat. Exp. Brain Res. 18 (1973) 131-144.

Rossini, P.M., Narich, L., Romani, G.L., Traversa, R., Cecchi, L., Cilli, M. and Urbano, A. Short latency somatosensory evoked responses to median nerve stimulation in healthy humans: electric and magnetic recordings. Int. J. Neurosci. 46 (1989) 67-76.

Sarvas, J. Basic mathematical and electromagnetic concepts of the biomagnetic inverse problem. Phys. Med. Biol. 32 (1987) 11-22.

Seyal, M., Emerson, R.G. and Pedley, T.A. Spinal and early scalp-recorded components of somatosensory evoked potential following stimulation of the posterior tibial nerve. Electroencephalogr. Clin. Neurophysiol. 55 (1983) 320-330.

Sherg, M. and Berg, P. BESA; Brain Electrical Source Analysis. Version 2.1. Handbook. Megis. Munich, Unpublished. (1995).

Shimojo, M., Kakigi, R., Hoshiyama, M., Koyama, S., Kitamura, Y. and Watanabe, S. Intracerebral interactions caused by bilateral median nerve stimulation in man: a magnetoencephalographic study. Neurosci. Res. 24 (1996a) 175-181.

Shimojo, M., Kakigi, R., Hoshiyama, M., Koyama, S., Kitamura, Y. and Watanabe, S. Differentiation of receptive fields in the sensory cortex following stimulation of various nerves of the lower limb in man. magnetoencephalographic study. J. Neurosurg. 85 (1996b) 255-262.

Shimojo, M., Kakigi, R., Hoshiyama, M., Koyama, S. and Watanabe, S. Magnetoencephalographic study of intracerebral interactions caused by bilateral posterior tibial nerve stimulation in man. Neurosci. Res. 28 (1997) 941-947.

Suk, J., Ribary, U., Cappell, J., Yamamoto, T. and Llinas, R. Anatomical localization revealed by MEG recordings of the human somatosensory system. Electroencephalogr. Clin. Neurophysiol. 78 (1991) 185-196.

Sutherling, W.W., Crandall, P.H., Darcey, T.M., Becker, D.P., Levesque, M.F. and Barth, D.S. The magnetic and electric fields agree with intracranial localizations of somatosensory cortex. Neurology, 38 (1988) 1705-1714.

Tiihonen, J., Hari. R. and Hämäläine, M. Early deflections of cerebral magnetic responses to median nerve stimulation. Electroencephalogr. Clin. Neurophysiol. 74 (1989) 290-296.

Tsuji, S. and Murai, Y. Variability of initial cortical sensory evoked potentials to posterior tibial nerve stimulation. JUOEH 9 (1987) 287-298.

Tsumoto, T., Hirose, N., Nonaka, S. and Takahashi, M. Analysis of somatosensory evoked potentials to lateral popliteal nerve stimulation in man. Electroencephalogr. Clin. Neurophysiol. 33 (1972) 379-388.

Wang, J., Cohen, L.G. and Hallett, M. Scalp topography of somatosensory evoked potentials following electrical stimulation of femoral nerve. Electroencephalogr. Clin. Neurophysiol. 74 (1989) 112-123.

Whitzel, B.L., Perrucelli, L. and Werner, G. Symmetry and connectivity in the body surface in somatosensory area II of primates. J. Neurophysiol. 32 (1969) 170-183.

Williamson, S.J. and Kaufman, L. Biomagnetism, J. Magn. Mat. 22 (1981) 129-202.

Wood, C.C., Cohen, D., Cuffin, B.N., Yarita, M. and Allison, T. Electrical sources in human somatosensory cortex: Identification by combined magnetic and potential recordings. Science, 227 (1985) 1051-1053.

Yamada, T., Kimura, J., Young, S. and Powers, M. Somatosensory-evoked potentials elecited by bilateral stimulation of the median nerve and its clinical application. Neurology, 28 (1978) 218-223.

Yamada, T., Machida, M. and Kimura, J. Far-field somatosensory evoked potentials after stimulation of the tibial nerve. Neurology, 32 (1982) 1151-1158.

Yamada, T., Kimura, J., Wilkinson, J.T. and Kayamori, R. Short- and long-latency median somatosensory evoked potentials. Findings in patients with localized neurological lesions. Arch. Neurol. 40 (1983) 215-220.

Yumoto, M., Okubo, A., Ugawa, Y. and Uesaka, Y. Source localization of the magnetic components corresponding to P22 following median nerve stimulation. Jpn. J. EEG EMG, 23 (1995) 182.

Table 1: Mean and standard deviation (S.D.) of peak latency (msec) of each recognizable component to each nerve stimulation.

	Left limb (n=7)	Right limb (n=7)	Total (n=14)
Posterior tibial nerve			
1M	36.8±3.2	37.2±2.6	37.0±2.8
2M	45.4±3.1	48.7±5.5	47.0±4.6
3M	57.6±3.3	58.7±6.2	58.2±4.8
4M	74.3±6.7	77.4±7.7	75.8±7.1
Sural nerve			
1M	38.8±3.4	39.0±3.3	38.9±3.2
2M	49.2±4.4	46.8±3.0	48.0±3.8
3M	60.1±6.8	60.9±5.0	60.5±5.7
4M	73.1±7.8	77.7±9.4	75.4±8.6
Peroneal nerve			
1M	29.4±1.6	30.7±4.3	30.0±3.2
2M	39.6±2.7	39.8±4.0	39.7±3.3
3M	48.8±3.9	49.4±4.8	49.1±4.2
4M	70.8±3.3	67.3±9.8	69.1±7.3
Femoral nerve			
1M	25.7±2.8	27.6±2.3	26.6±2.7
2M	34.0±1.9	37.2±3.2	35.6±2.6
3M	48.4±4.8	51.0±6.7	49.7±5.8
4M	65.4±7.4	69.4±11.5	67.4±9.5

Table 2: Comparison of peak latencies among different nerve stimulation.

1M: Sural>Tibial***, Tibial>Peroneal***, Tibial>Femoral***,
Sural>Peroneal***, Sural>Femoral***, Peroneal>Femoral*

2M: Tibial>Peroneal***, Sural>Peroneal***, Sural>Femoral***,

3M: Tibial>Peroneal***, Tibial>Femoral**, Sural>Peroneal***,
Sural>Femoral***,

4M: Tibial>Peroneal*, Tibial>Femoral**, Sural>Femoral*

Only the results that showed a significant difference by paired t test are given.
($P<0.02$*, $P<0.01$**, $P<0.001$***)

Table 3: Mean and standard deviation (S.D.) of amplitude (fT) of each recognizable component to each nerve stimulation.

	Left limb (n=7)	Right limb (n=7)	Total (n=14)
Posterior tibial nerve			
1M	361.4±106.0	318.6±82.7	340.0±94.0
2M	230.0±71.9	203.6±64.3	216.8±67.0
3M	215.0±81.7	253.6±77.0	234.3±78.7
4M	317.1±114.7	253.6±143.1	285.4±128.9
Sural nerve			
1M	215.7±44.9	210.0±81.4	212.9±63.2
2M	190.7±127.1	232.1±66.7	211.4±99.9
3M	179.3±34.5	165.0±42.5	172.1±37.9
4M	202.1±71.0	197.9±81.7	200.0±73.6
Peroneal nerve			
1M	167.9±62.8	160.0±68.8	163.9±63.4
2M	195.7±95.0	218.6±104.3	207.1±96.6
3M	188.6±90.0	156.4±33.3	172.5±67.1
4M	199.3±47.6	205.0±48.1	202.1±46.1
Femoral nerve			
1M	133.6±54.8	158.6±58.6	146.1±56.0
2M	141.4±71.7	177.1±74.2	159.3±72.5
3M	152.1±50.9	140.0±61.1	146.1±54.4
4M	190.7±91.5	203.6±55.1	197.1±72.9

Table 4: Comparison of amplitudes among different nerve stimulation.

1M: Tibial>Sural***, Tibial>Peroneal***, Tibial>Femoral***,
Sural>Femoral*,

2M: Tibial>Femoral*, Sural>Femoral**,

3M: Tibial>Sural*, Tibial>Femoral***, Sural>Peroneal****,

4M: Tibial>Sural*, Tibial>Peroneal*,

Only the results that showed a significant difference by paired t test are given. ($P<0.02$*, $P<0.01$**, $P<0.001$***)

Table 5: Distance of ECDs (cm) between each nerve stimulation.

	Left limb (n=7)	Right limb (n=7)	Total (n=14)
Posterior tibial - Sural			
1M	0.72±0.43	1.24±0.54	0.98±0.54
2M	1.31±0.72	1.21±0.75	1.26±0.71
3M	2.02±0.61	1.71±0.76	1.86±0.68
4M	1.13±0.76	1.85±0.65	1.49±0.78
Posterior tibial - Peroneal			
1M	0.79±0.44	1.37±0.66	1.08±0.61
2M	1.55±0.90	1.94±1.41	1.75±1.15
3M	1.65±1.12	1.85±1.00	1.75±1.02
4M	0.93±0.52	2.52±0.74	1.73±1.03
Posterior tibial - Femoral			
1M	1.43±0.58	1.31±0.82	1.37±0.69
2M	1.43±0.43	1.69±0.59	1.56±0.52
3M	1.71±0.62	1.57±0.45	1.64±0.53
4M	1.57±0.47	2.16±0.82	1.86±0.71
Sural - Peroneal			
1M	0.90±0.26	1.50±0.64	1.20±0.56
2M	1.94±0.48	1.41±0.57	1.67±0.58
3M	2.19±0.33	2.06±0.51	2.13±0.42
4M	1.50±0.76	2.01±0.43	1.76±0.65

Sural - Femoral

1M	1.70±0.56	1.73±0.77	1.71±0.64
2M	1.97±0.58	2.03±0.68	2.00±0.61
3M	1.87±1.11	1.54±0.69	1.70±0.91
4M	1.37±0.47	2.42±0.67	1.89±0.78

Peroneal - Femoral

1M	1.12±0.55	1.70±0.65	1.41±0.65
2M	1.54±1.13	2.06±1.03	1.80±1.07
3M	2.46±1.54	2.05±1.30	2.26±1.38
4M	1.45±0.91	2.84±0.93	2.15±1.14

Significant difference was found by paired t test between
1M: (Tibial - Sural) and (Sural - Femoral) -- $P<0.001$
(Tibial - Sural) and (Peroneal - Femoral) -- $P<0.01$
2M: (Tibial - Sural) and (Sural - Femoral) -- $P<0.001$
3M: (Tibial - Femoral) and (Sural - Peroneal) -- $P<0.01$

Table 6: Distance of ECDs (cm) between each nerve stimulation in type 1 and type 2.

	Type 1 (n=9)	Type 2 (n=5)
Posterior tibial - Sural		
1M	0.98±0.52	1.10±0.71
2M	1.32±0.64	1.33±0.82
3M	1.97±0.57	1.51±0.82
4M	1.32±0.78	1.64±0.58
Posterior tibial - Peroneal		
1M	0.75±0.53	1.43±0.63
2M	1.58±0.88	2.34±1.46
3M	1.60±1.07	2.35±0.52
4M	1.47±1.04	2.44±0.97
Posterior tibial - Femoral		
1M	1.76±0.47	0.65±0.23
2M	1.51±0.48	1.82±0.62
3M	1.56±0.33	1.82±0.79
4M	1.97±0.89	1.97±0.76
Sural - Peroneal		
1M	1.12±0.48	1.47±0.75
2M	1.82±0.58	1.63±0.34
3M	2.15±0.29	2.08±0.62
4M	1.44±0.50	2.36±0.44

Sural - Femoral

1M	1.93±0.45	1.35±0.84
2M	1.98±0.59	2.25±0.60
3M	1.34±0.96	2.22±0.73
4M	1.85±0.81	1.87±0.65

Peroneal - Femoral

1M	1.39±0.54	1.64±0.89
2M	1.65±1.18	2.59±0.67
3M	1.75±1.25	3.18±1.19
4M	1.45±0.95	3.00±0.71

Significant difference was found by paired t test in type 1 between

1M: (Tibial - Sural) and (Tibial - Femoral) -- $P<0.01$
(Tibial - Sural) and (Sural - Femoral) -- $P<0.01$
(Tibial - peroneal) and (Tibial - Femoral) -- $P<0.01$
(Tibial - peroneal) and (Sural - Femoral) -- $P<0.01$
(Tibial - Femoral) and (Sural - Peroneal) -- $P<0.01$
(Tibial - Femoral) and (Peroneal - Femoral) -- $P<0.01$
(Sural - Peroneal) and (Sural - Femoral) -- $P<0.01$
(Sural - Femoral) and (Peroneal - Femoral) -- $P<0.001$
2M: (Tibial - Sural) and (Sural - Peroneal) -- $P<0.02$
(Tibial - Femoral) and (Sural - Femoral) -- $P<0.01$
(Tibial - Sural) and (Sural - Femoral) -- $P<0.02$
3M: (Tibial - Femoral) and (Sural - Peroneal) -- $P<0.001$

No significant difference was found in type 2.

Table 7: Peak latencies of each identifiable component of "summated" waveform and "bilateral" waveform (mean ±S.D. in msec).

	"Summated"	"Bilateral"
N20m-P20m		
C3	18.5±1.4	18.4±1.2
C4	18.7±2.0	18.8±2.1
C3+C4	18.6±1.7	18.6±1.6
N30m-P30m		
C3	28.3±6.0	28.5±6.1
C4	28.2±5.5	28.2±5.6
C3+C4	28.2±5.6	28.4±5.6
N40m-P40m		
C3	41.1±9.1	42.2±9.3
C4	41.9±7.0	41.9±8.0
C3+C4	41.5±7.9	42.1±8.4
N60m-P60m		
C3	65.0±12.3	64.2±12.6
C4	64.1±11.0	64.3±11.7
C3+C4	64.5±11.3	64.3±11.6
N90m-P90m		
C3	100.4±16.1	98.9±17.0
C4	95.3±19.5	93.3±18.6
C3+C4	97.9±17.4	96.1±17.3

Summated: Summated waveform, Bilateral: Bilateral waveform, C3 and C4: Results recorded when the magnetometer was placed at the C3 and C4 positions, respectively. C3+C4: Simple summation of results acquired in "C3" and "C4" sessions. The number of subjects was 7 in the C3 and C4 sessions, and 14 in the "C3+C4"session. There was no significant difference between the "summated" and "bilateral" waveform.

Table 8: Amplitudes of each identifiable component of "summated" waveform and "bilateral" waveform (mean ±S.D. in fT).

	"Summated"	"Bilateral"
N20m-P20m		
C3	417.1±192.8	430.0±187.8
C4	432.9±317.1	412.9±300.4
C3+C4	425.0±252.2	421.4±240.9
N30m-P30m		
C3	411.4±248.2	397.1±184.5
C4	520.0±180.5	460.0±147.5
C3+C4	465.7±215.9	428.6±163.8
N40-P40m		
C3	215.7±147.6	217.2±127.7
C4	170.7±79.5	157.2±69.7
C3+C4	203.2±157.7	195.4±98.5
N60m-P60m		
C3	540.0±204.5	485.7±181.0
C4	374.3±118.3	227.1±101.6*
C3+C4	452.1±182.4	355.7±194.6
N90m-P90m		
C3	461.4±146.2	290.0±111.1*
C4	340.0±126.4	235.7±73.7*
C3+C4	402.1±144.5	267.1±94.1**

Summated: Summated waveform, Bilateral: Bilateral waveform. The amplitude was measured by adding the maximum amplitude of the outgoing and ingoing fluxes. For example, "amplitude of N20m- P20m" was obtained by adding the maximum amplitude of N20m and that of P20m. Differences between the "summated" and "bilateral" waveform were anlyzed using paired t test (*$P<0.01$, **$P<0.001$).

Table 9: Peak latencies (msec) and amplitudes (fT) of each identifiable component of "summated" waveform and "bilateral" waveform (mean ± S.D.). The number of subjects was seven.

		"Summated"	"Bilateral"
N37m-P37m	Latency	37.4 ± 2.1	37.7 ± 2.6
	Amplitude	350.3 ± 163.5	345.6 ± 170.2
N45m-P45m	Latency	47.6 ± 5.4	47.3 ± 5.0
	Amplitude	393.6 ± 253.9	335.3 ± 159.9
N60m-P60m	Latency	62.3 ± 7.0	62.7 ± 5.9
	Amplitude	336.4 ± 167.5	329.0 ± 180.5
N75m-P75m	Latency	78.0 ± 8.1	74.7 ± 6.7
	Amplitude	272.6 ± 107.8	237.4 ± 81.5
N100m-P100m	Latency	99.8 ± 13.1	99.3 ± 12.2
	Amplitude	345.1 ± 117.4	265.4 ± 96.4*

Summated: Summated waveform, Bilateral: Bilateral waveform, The amplitude was measured by adding the maximum amplitude of the outgoing and ingoing flux. For example, in "amplitude of N37m-37m" the maximum amplitude of the N37m and that of the P37m was added. Statistical analysis was done between "summated" and "bilateral" waveform by paired t test, and the amplitude difference of N100m-P100m was significant (*$P<0.02$).

Legends for Figures

Fig. 1: SEFs following stimulation of the posterior tibial and the sural nerve at the ankle, peroneal nerve at the knee and the femoral nerve overlying the inguinal ligament of the right lower limb in the first participant. Waveforms recorded at the 37 channels were superimposed. Four components, 1M, 2M, 3M and 4M, were identified in each waveform. They were labeled in the waveform following posterior tibial nerve stimulation, and were indicated by the arrows in the other waveforms. Minor deflection indicated by * was identified in the waveform following stimulation of the posterior tibial and the sural nerve stimulation.

Fig. 2: Isocontour maps of the 1M following stimulation of the posterior tibial, sural, peroneal and femoral nerve of the right limb in the second participant. Contour step was 10, 5, 5 and 10 fT in waveforms of the posterior tibial, sural, peroneal and femoral nerve stimulation, respectively. The dotted line and the thin line indicated the ingoing and outgoing flux, respectively, and the thick line indicated the zero-point line. The center of the map was around the vertex (Cz of the International 10-20 System). "A", "P", "L" and "R" in the map following stimulation of the posterior tibial nerve indicated the orientation of the map; anterior, posterior, left and right, respectively. The magnetic field following the femoral nerve stimulation was much different from those of the other nerves stimulation.

Fig. 3: Location and direction of ECDs of the 1M following stimulation of the posterior tibial, sural, peroneal and femoral nerves of the right limb overlapped on axial and coronal views of MRI in the second participant, based on Fig. 2. "R" and "L" in the MRI following posterior tibial nerve stimulation means the right and left direction, respectively. The ECD following the femoral nerve stimulation was located on the crown of the postcentral gyrus directed to inferior and posterior side. However, the ECDs following stimulation of the other nerves were located along the interhemispheric fissure directed to the right hemisphere. Their ECDs were located very close to each other, but that following peroneal nerve stimulation was slightly higher than the other 2 nerve stimulations. This type of receptive field was classified into type 1.

Fig. 4: Isocontour maps of the 1M following stimulation of the posterior tibial, sural, peroneal and femoral nerve of the left limb in the third participant. Contour step was 10, 5, 2 and 5 fT in waveform of the posterior tibial, sural, peroneal and femoral nerve stimulation, respectively. The dotted line and the thin line indicated the ingoing and outgoing flux, respectively, and the thick line indicated the zero-point line. The center of the map was around the vertex (Cz of the International 10-20 System). A, P, L and R in the map following stimulation of the posterior tibial nerve indicated the orientation of the map; anterior, posterior, left and right, respectively. Magnetic fields following posterior tibial and sural nerve stimulation were similar. However, those following peroneal and femoral nerves were much different from those following stimulation of the posterior tibial and sural nerve. Notice the inverted magnetic fields between peroneal and femoral nerve stimulation.

Fig. 5: Location and direction of ECDs of the 1M following stimulation of the posterior tibial, sural, peroneal and femoral nerves of the left limb overlapped on axial and coronal views of MRI in the third participant, based on Fig. 4. "R" and "L" in the MRI following posterior tibial nerve stimulation mean the right and left direction, respectively. The ECDs following stimulation of each nerve were located close to each other, along the interhemispheric fissure. Those following stimulation of the posterior and sural nerve were directed to the right hemisphere horizontally, but that following stimulation of the peroneal and femoral nerves directed anteriorly and posteriorly, respectively. This type of receptive field was classified into type 2.

Fig. 6: SEFs of the two representative positions which were recorded at the C3 position in one subject, showing nomenclature of each identifiable component.

Fig. 7: Localization of representative ECDs of N20m-P20m in the "bilateral" and "summated" waveforms recorded at the C3 position overlapped on axial and coronal views of MRI in one subject. They were located on the hand area of SI in the left hemisphere.

Fig. 8: The "bilateral", "summated" and "difference" waveforms recorded at the C3 position in one subject. Each waveform was obtained by superimposition of all 37 channels. The N90m-P90m in the "bilateral" waveform was smaller than those in the "summated" waveform, and U90m-D90m was found in the difference waveform.

Fig.9: Localization of representative ECDs of the N90m-P90m in the "bilateral" and "summated" waveforms, and that of the U90m- D90m in the "difference" waveforms recorded at the C3 position overlapped on axial and

coronal views of MRI in one subject. They were located on the hand area of SII in the left hemisphere.

Fig. 10: The "summated", "bilateral" and "difference" waveforms when the magnetometer was centered at the Cz position. Each waveform was obtained by superimposition of 37 channels. There was no significant difference between the "bilateral" and "summated" waveform, and no consistent deflection was found in the "difference" waveform.

Fig. 11: SEFs of the two representative positions following stimulation of the right posterior tibial nerve in subject one showing nomenclature of each identifiable component. The magnetometer was centered around the Cz position.

Fig. 12: The "summated", "bilateral" and "difference" waveforms recorded in subject one and two. Each waveform was obtained by superimposition of all 37 channels. The magnetometer was centered around the Cz position. The N100m-P100m in the "bilateral" waveform was smaller than those in the "summated" waveform, and the U100m-D100m was found in the difference waveform.

Fig. 13: Localization of two ECDs of the N37m-P37m estimated by using double ECD model in the "bilateral" waveforms overlapped on MRI in subject one and three. The magnetometer was centered around the Cz position. They were located in the foot area of SI in each hemisphere in both subjects. In type 1 (subject one), the ECDs in the two hemispheres were over 1 cm apart. However, in type 2 (subject three), the ECDs in the two hemispheres were very close to each other less than 1 cm, and were in exactly the opposite direction. The isocontour maps indicated the difference between type 1 and

type 2 more clearly. The maps in type 1 clearly depicted two dipoles, but those in type 2 did not. The maps in type 2 rather revealed a single ECD with small amplitude. A, P, L and R in the map indicated the orientation of the map; anterior, posterior, left and right, respectively. Contour step was 10 fT and 20 fT in subject one and three, respectively.

Fig. 14: Localization of two ECDs of the N100m-P100m estimated by using double ECD model in the "summated" and "bilateral" waveforms, overlapped on MRI in subject one. The magnetometer was centered around the Cz position. They were located along the superior bank of the Sylvian fissure, probably in SII in both hemispheres. Contour step was 20 fT.

Fig. 1

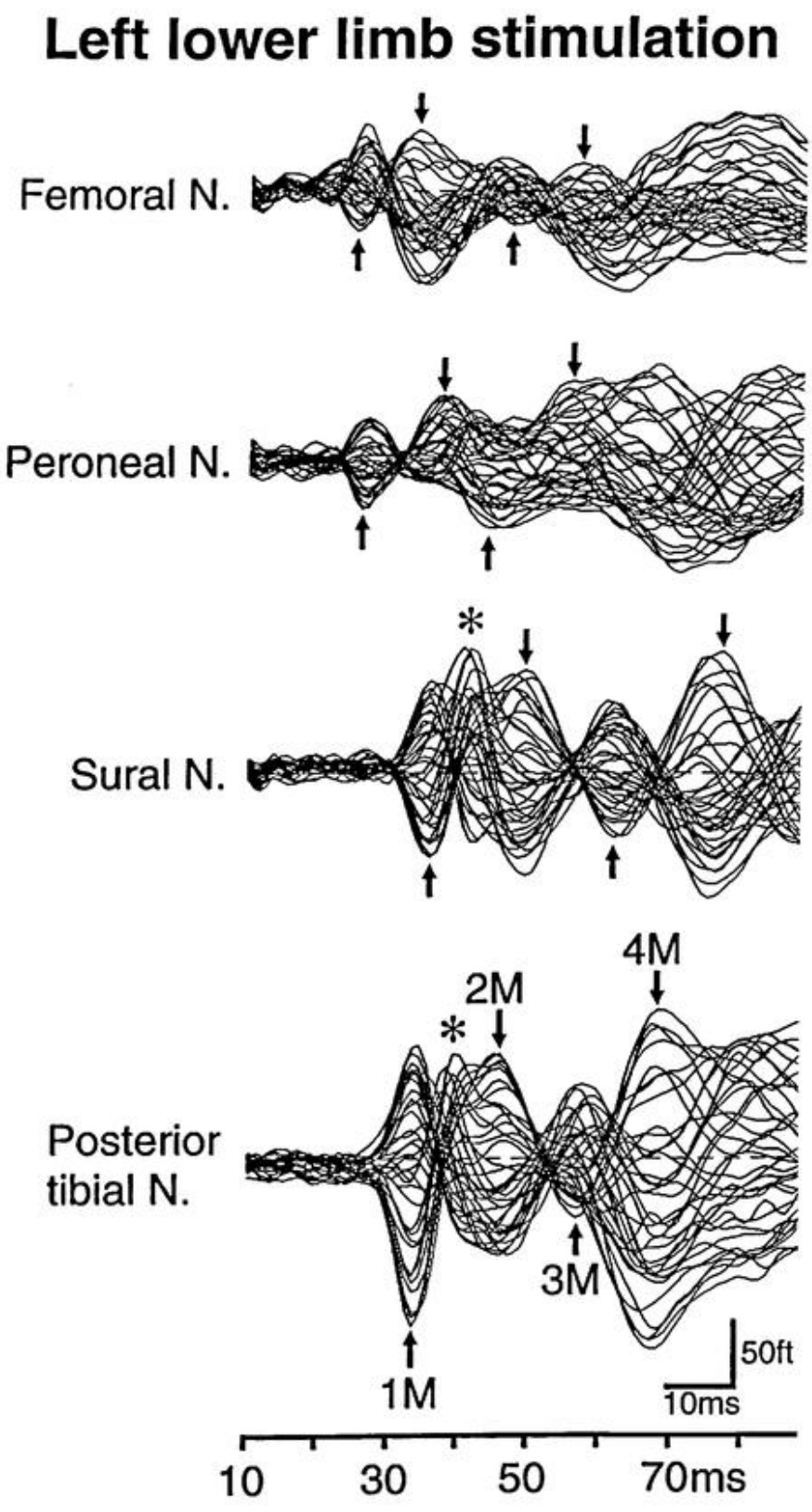
Left lower limb stimulation
Femoral N.
Peroneal N.
Sural N.
Posterior tibial N.
*
*
2M
4M
3M
1M
50ft
10ms
10
30
50
70ms

Fig. 2

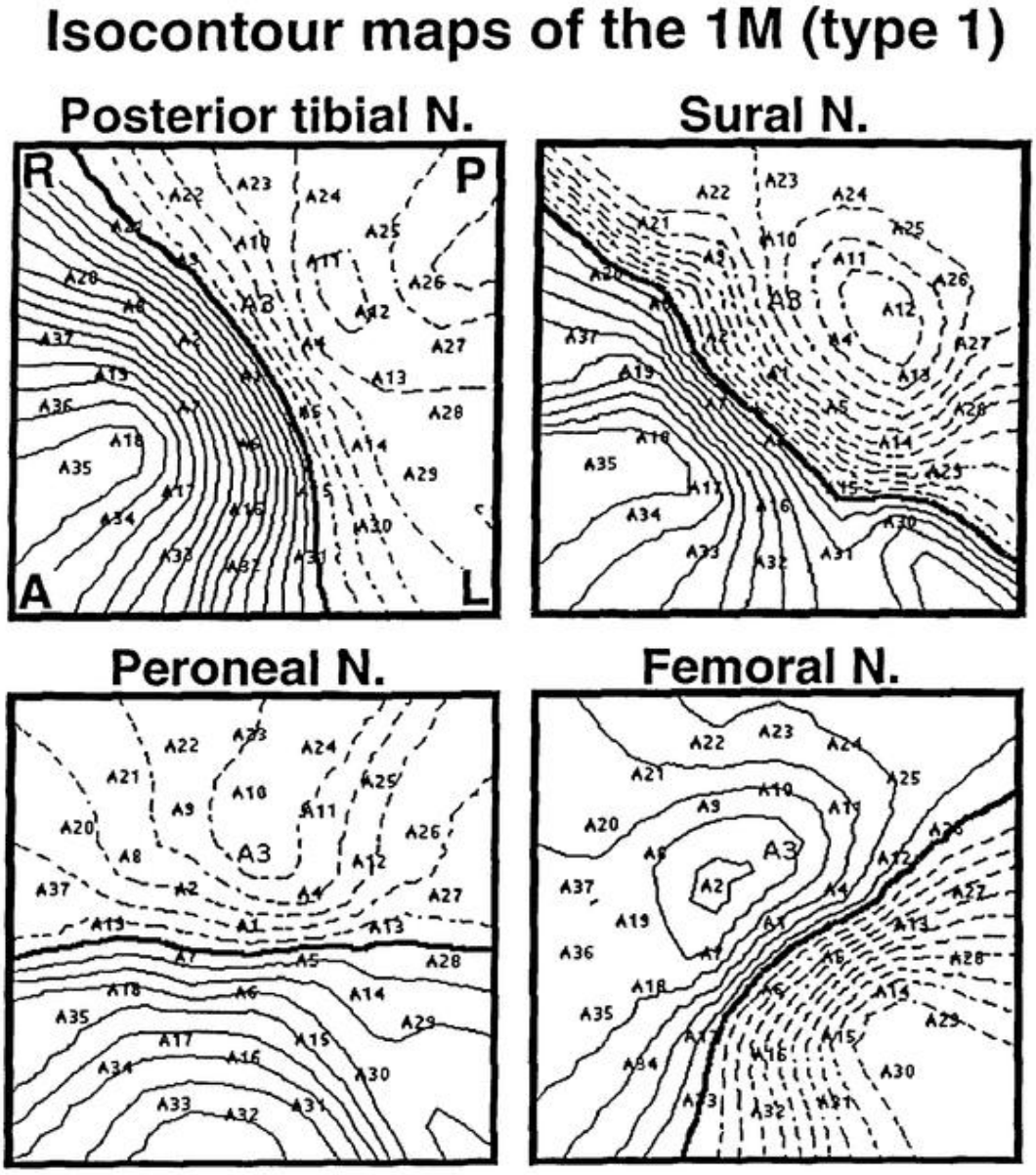
Isocontour maps of the 1M (type 1)
Posterior tibial N.
Sural N.
Peroneal N.
Femoral N.
R
P
A
L

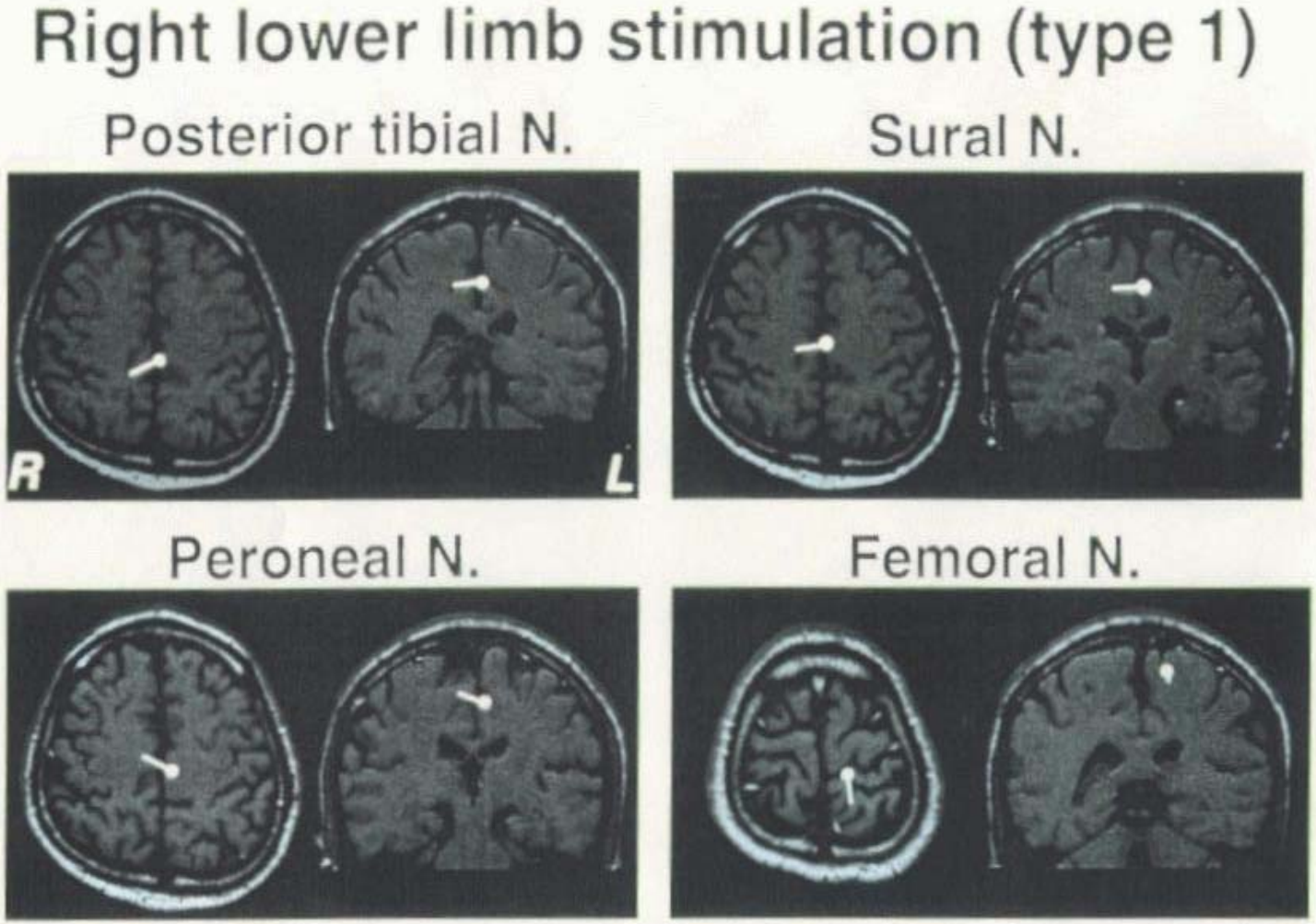
Right lower limb stimulation (type 1)
Posterior tibial N.
Sural N.
R
L
Peroneal N.
Femoral N.

Fig. 3

Fig. 4

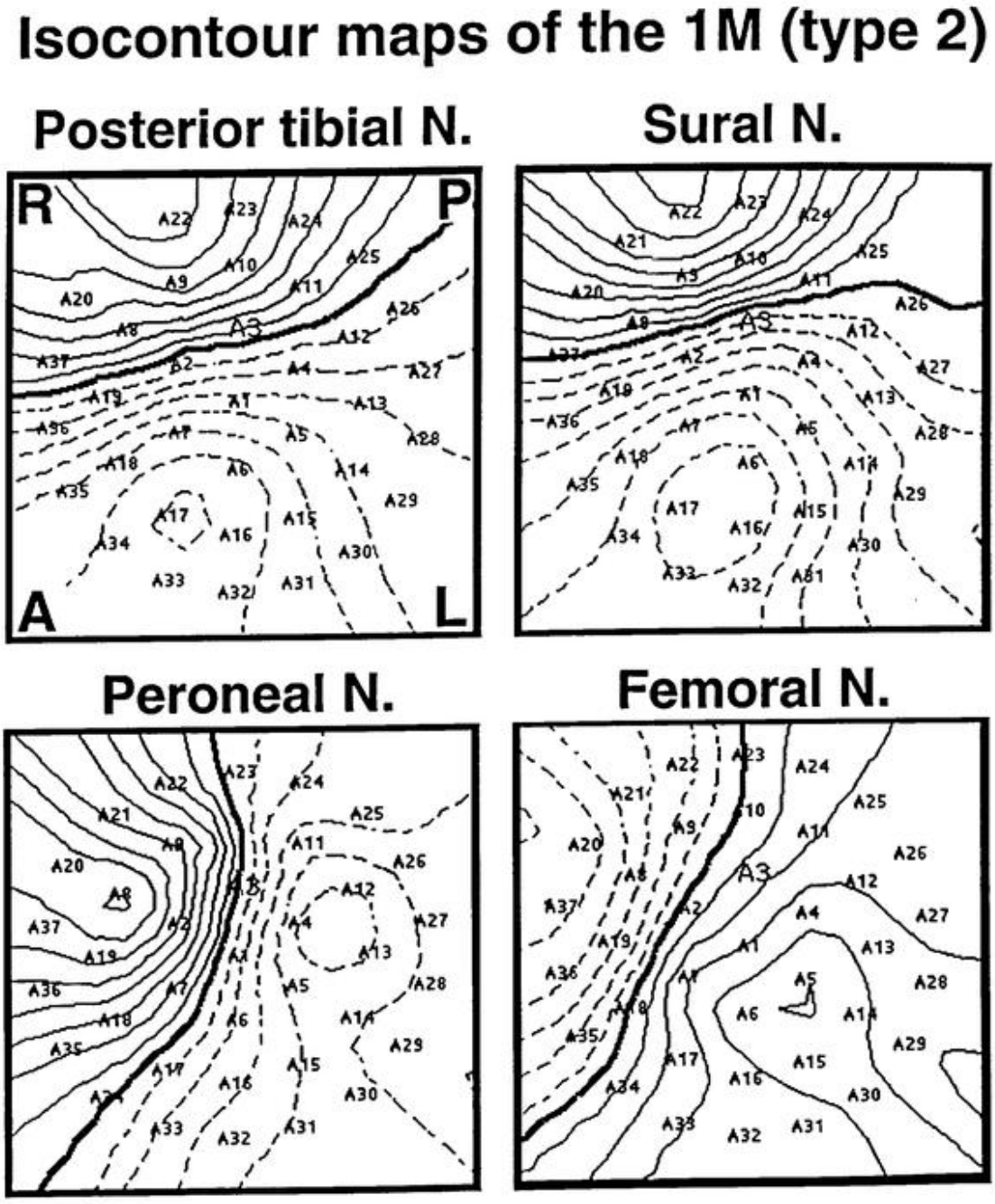
Isocontour maps of the 1M (type 2)
Posterior tibial N.
Sural N.
Peroneal N.
Femoral N.
R
P
A
L

Fig. 5

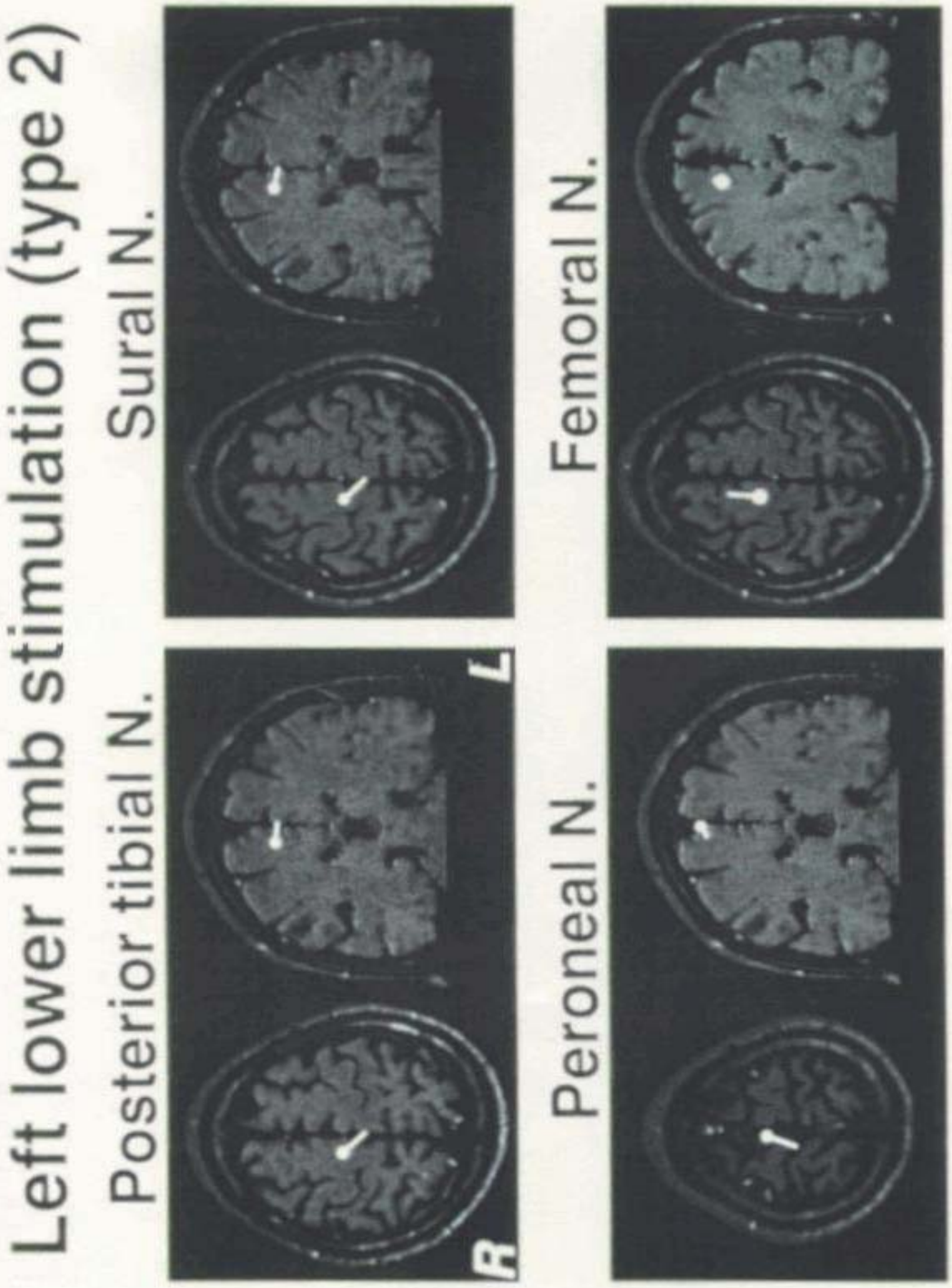
Left lower limb stimulation (type 2)
Posterior tibial N.
Sural N.
Peroneal N.
Femoral N.
R
L

Fig. 6

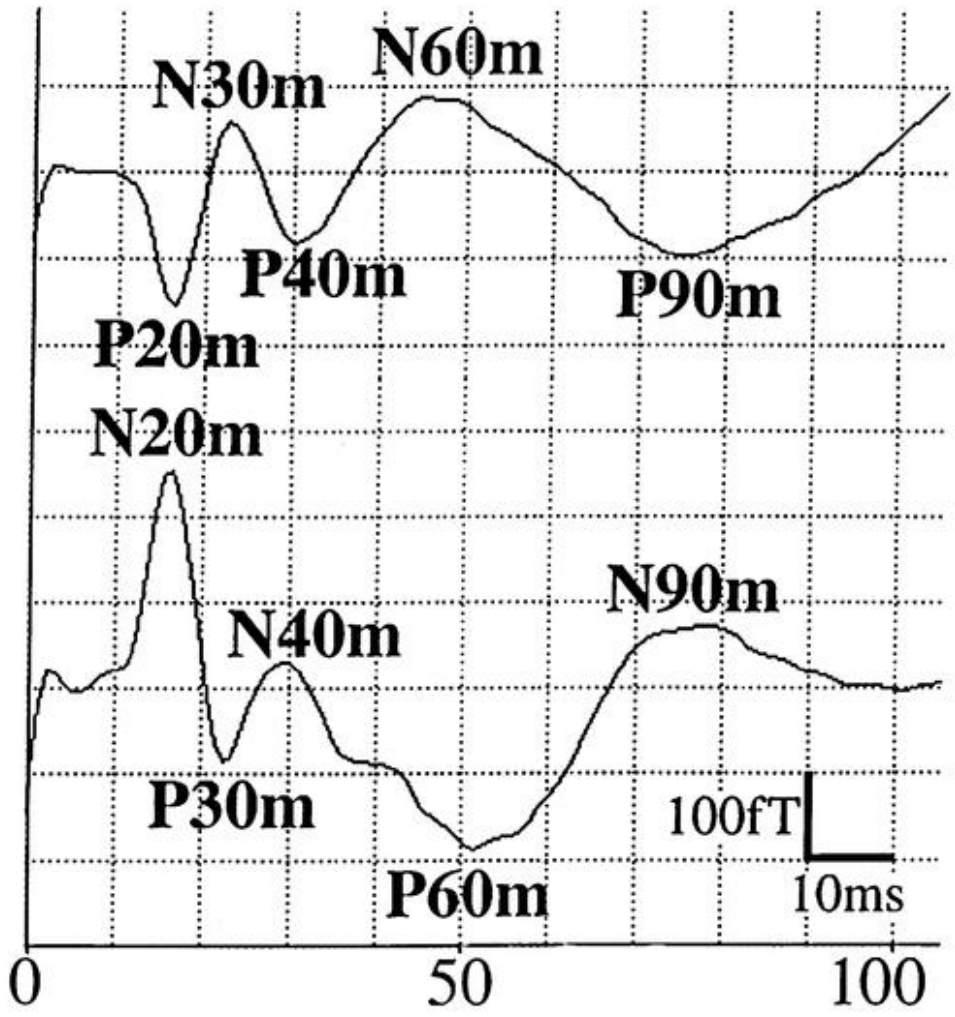
N30m
N60m
P40m
P90m
P20m
N20m
N90m
N40m
P30m
100fT
10ms
P60m
0
50
100

Fig. 7

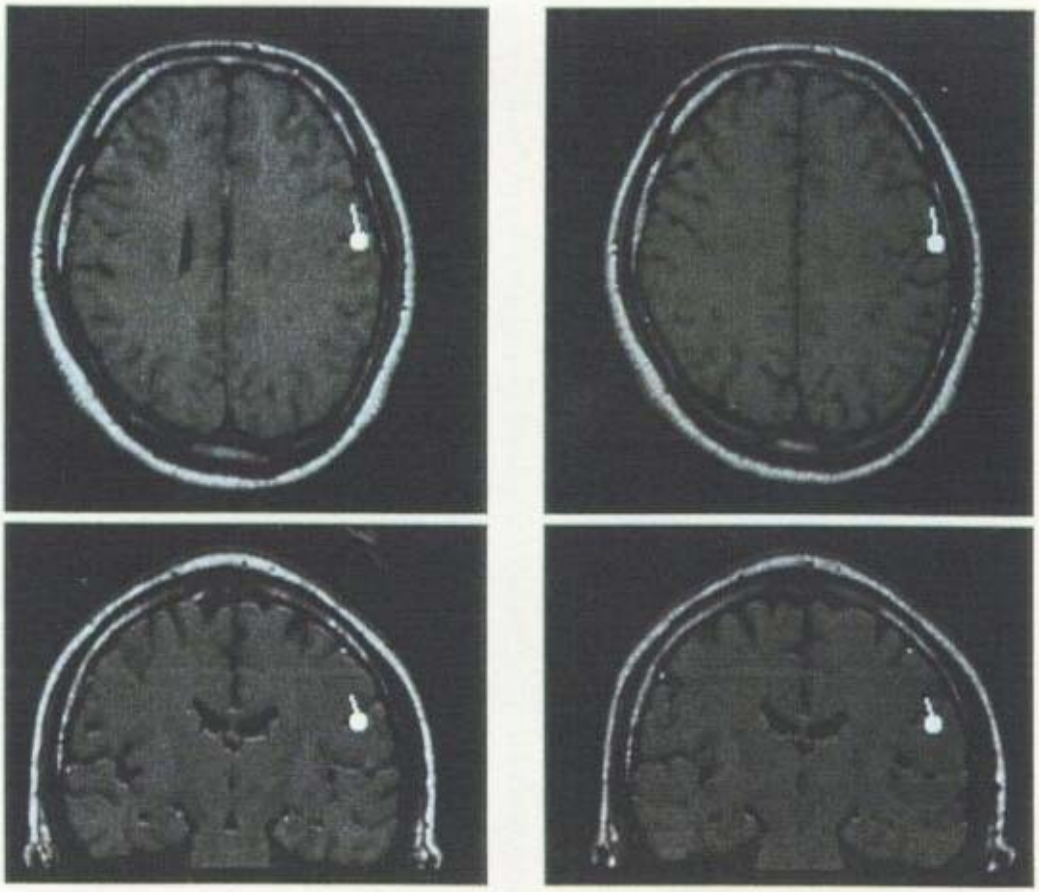

summated N20m-P20m

bilateral N20m-P20m

Fig. 8

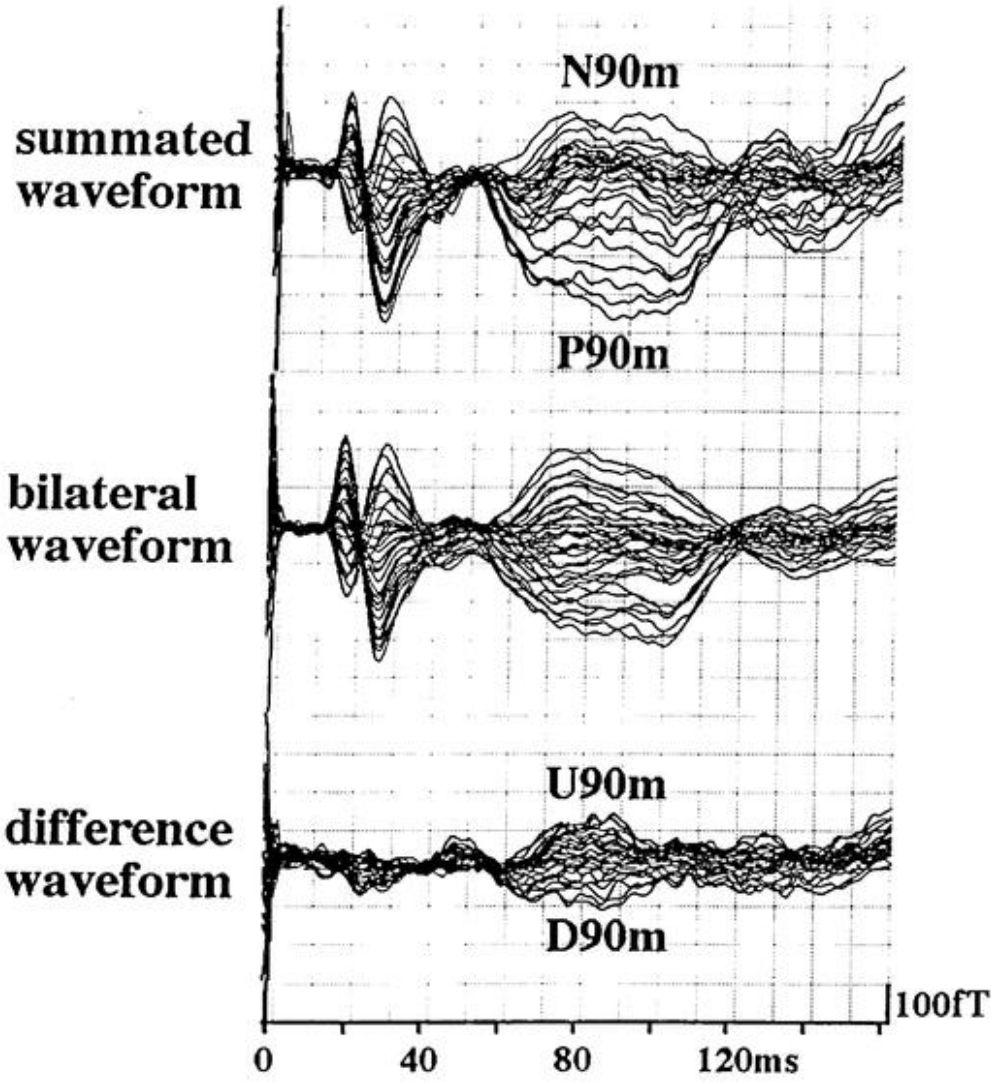
summated waveform
N90m
P90m
bilateral waveform
difference waveform
U90m
D90m
100fT
0
40
80
120ms

Fig. 9

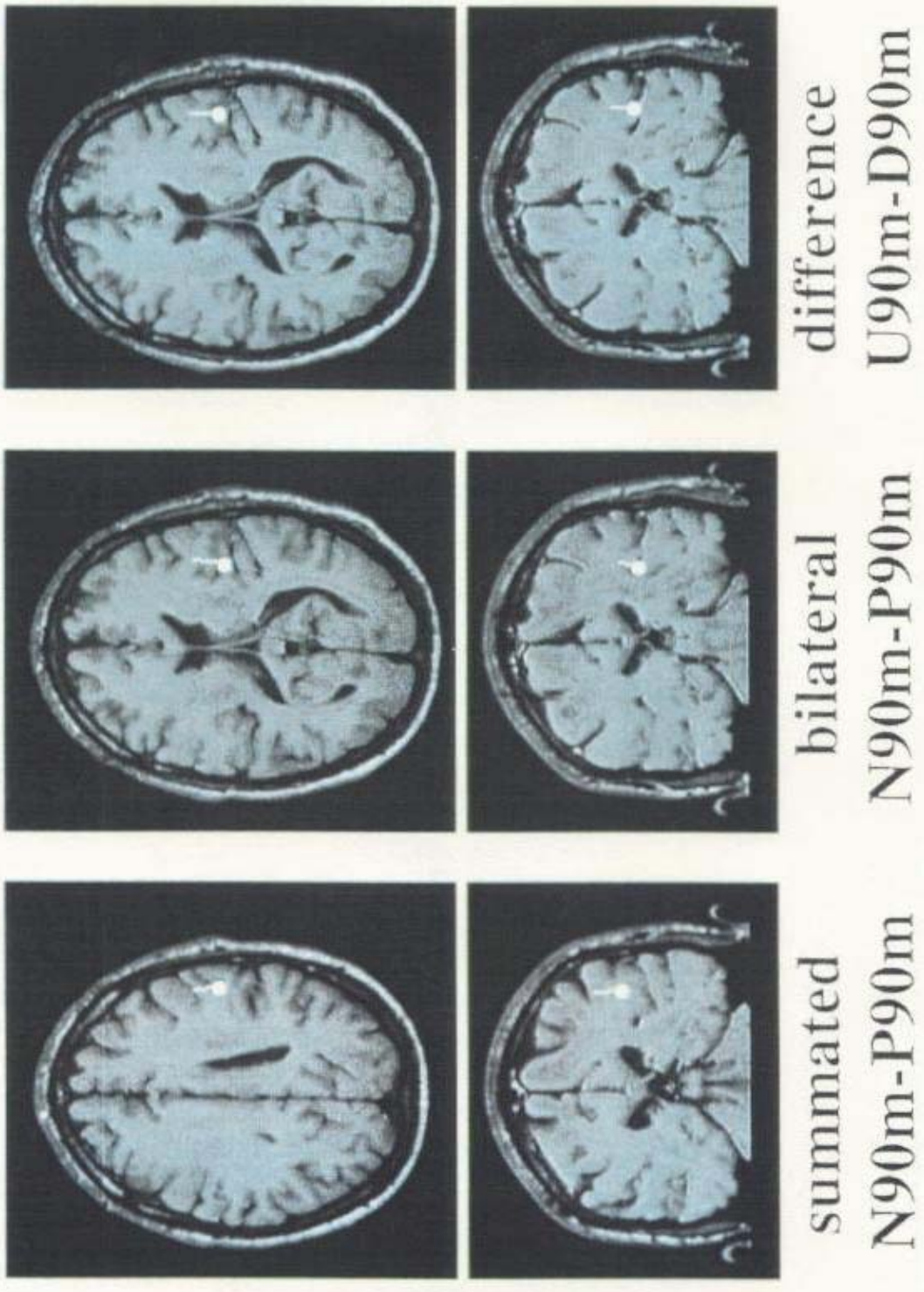
summated
N90m-P90m
bilateral
N90m-P90m
difference
U90m-D90m

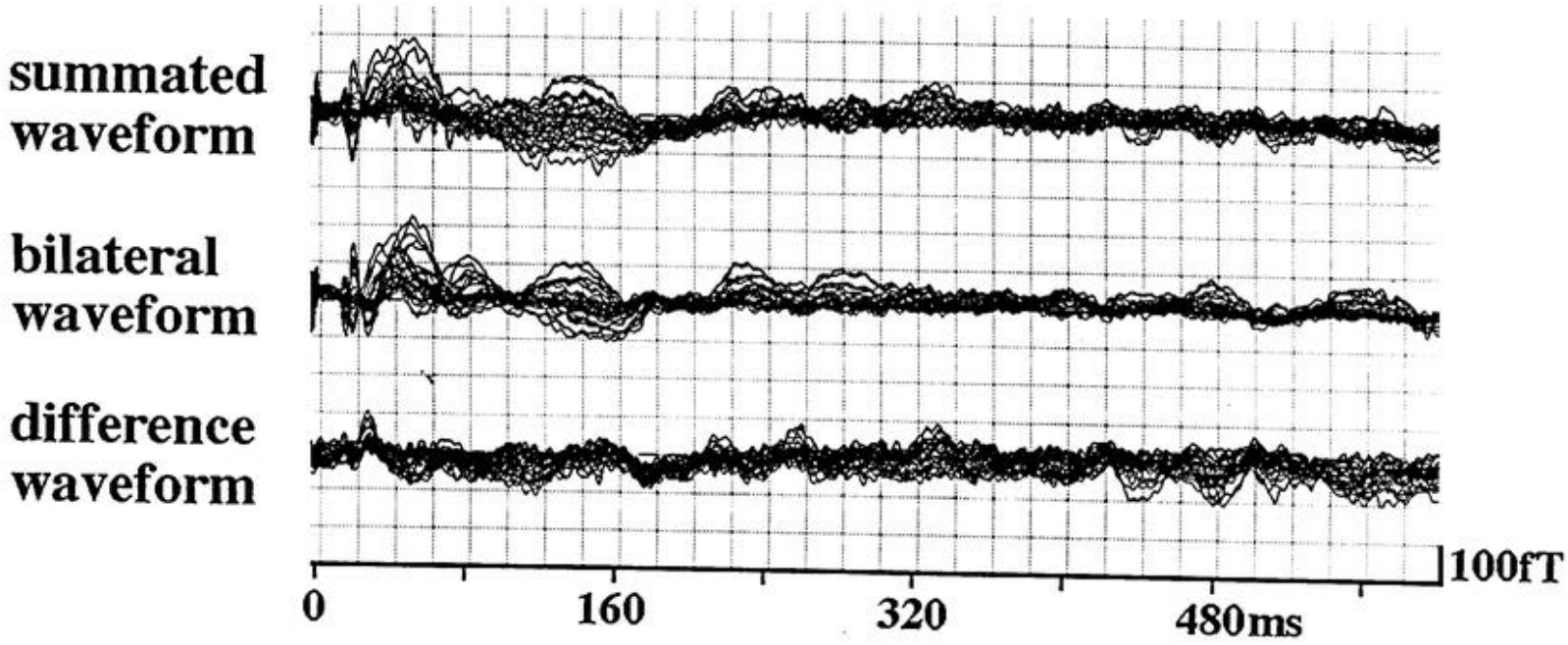
summated waveform
bilateral waveform
difference waveform
100fT
0
160
320
480ms

Fig. 10

Fig. 11

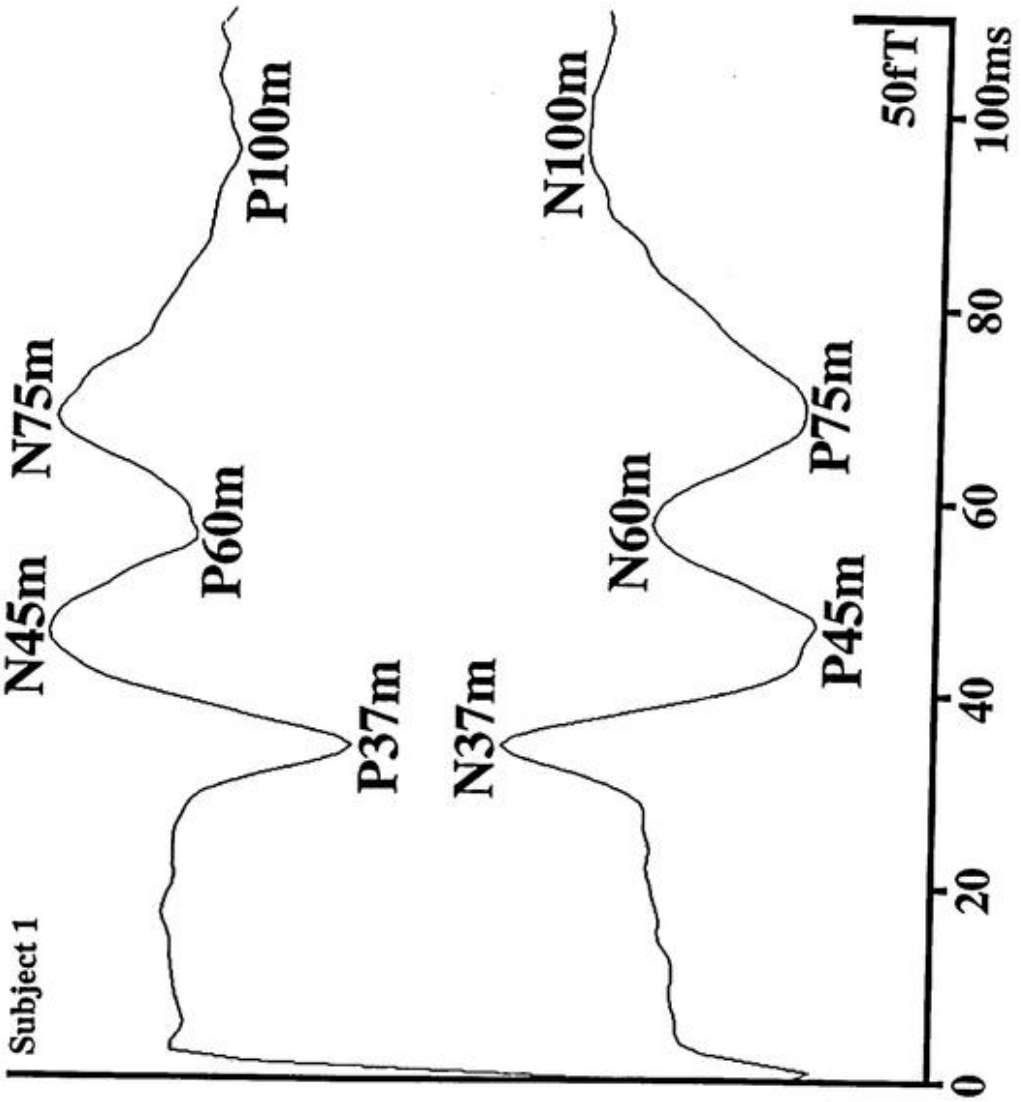
Subject 1
N45m
N75m
P100m
P60m
P37m
N37m
N100m
N60m
P75m
P45m
0
20
40
60
80
100ms
50fT

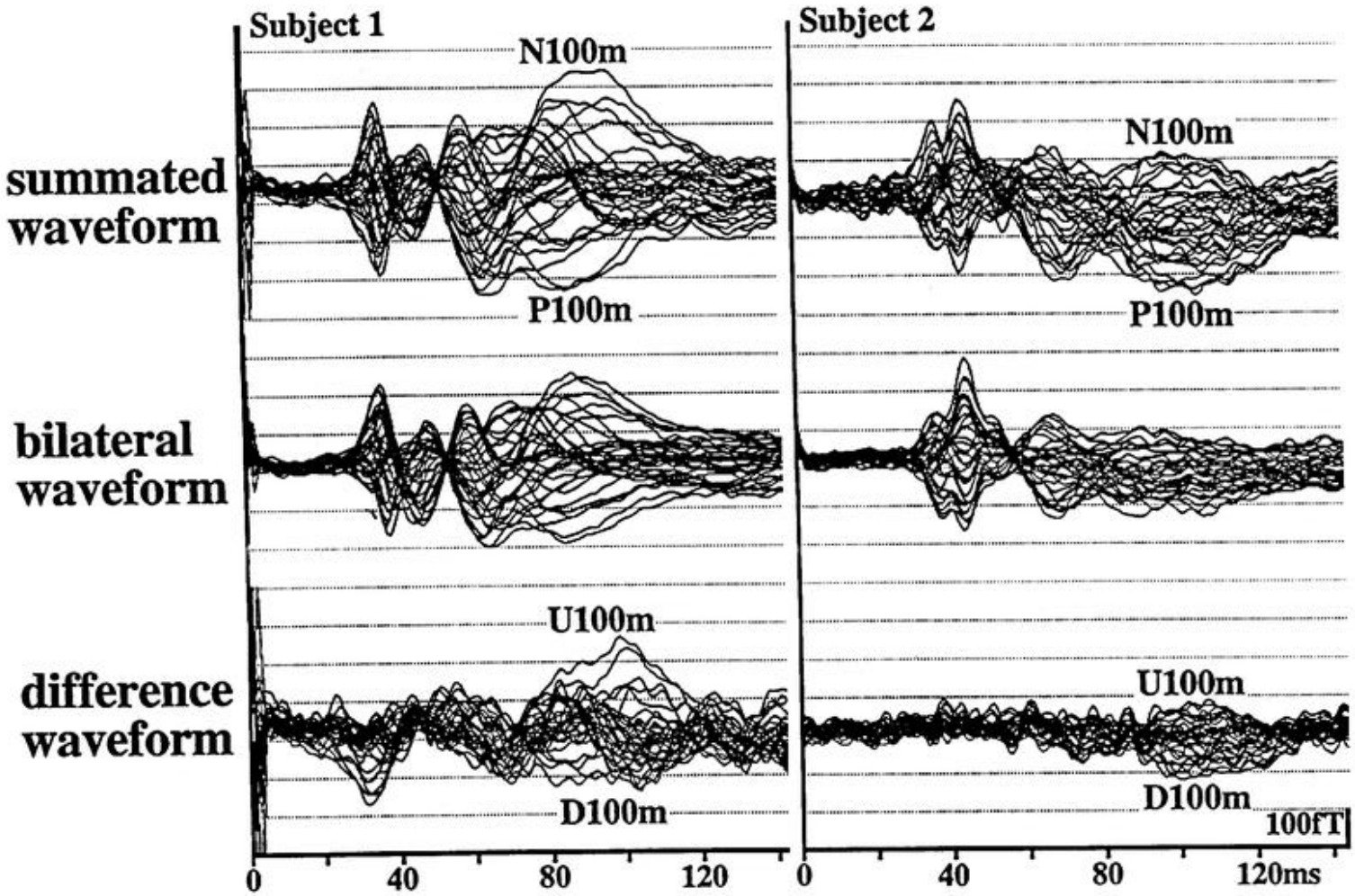
Subject 1
Subject 2
N100m
P100m
summated waveform
bilateral waveform
U100m
D100m
difference waveform
100fT
0
40
80
120
120ms

Fig. 12

Fig. 13

N37m-P37m (bilateral waveform)

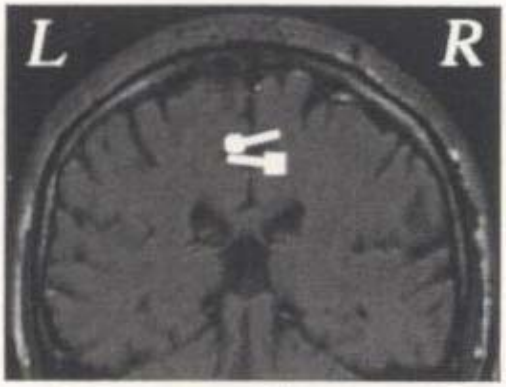

Type 1 Subject 1

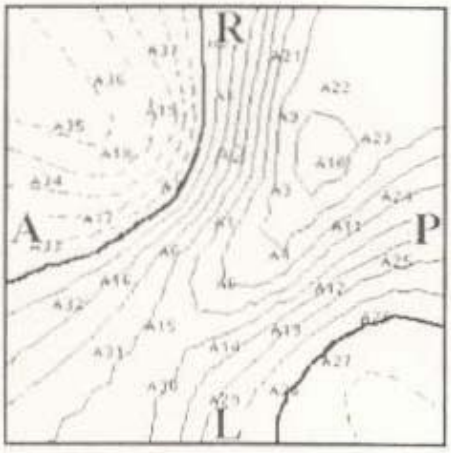

Type 2 Subject 3

N100m-P100m

Subject 1

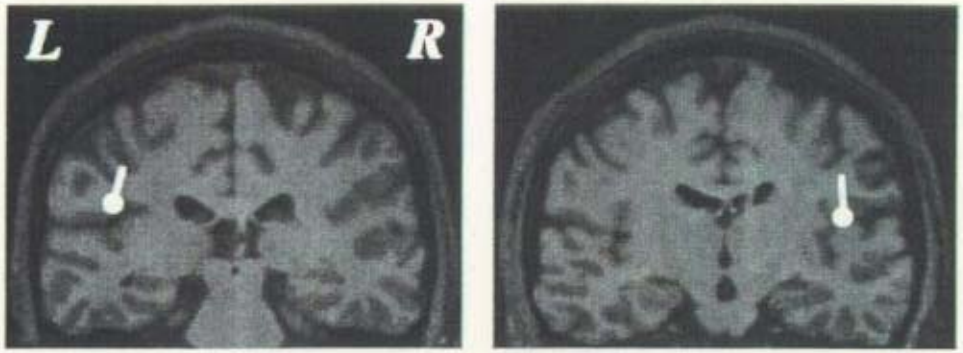

summated waveform

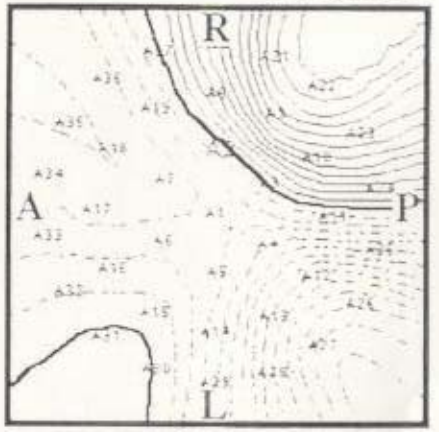

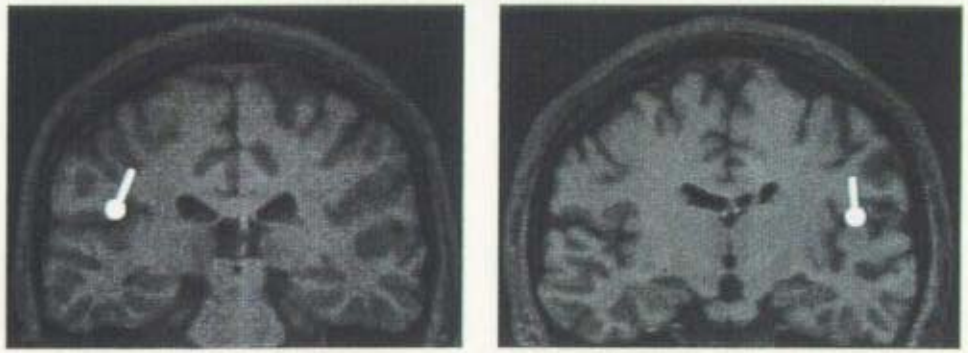

bilateral waveform

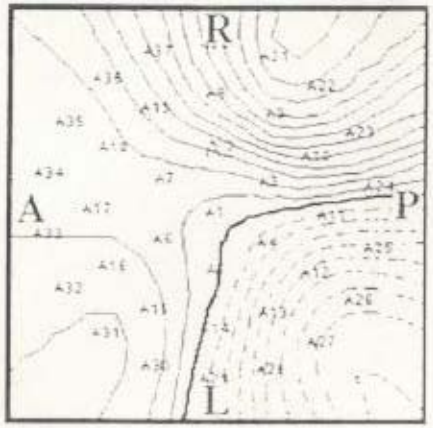

Fig. 14